Journal of Visualized Experiments

Optimization, test and diagnostics of miniaturized Hall thrusters

--Manuscript Draft--

Article Type:	Invited Methods Collection - Author Produced Video
Manuscript Number:	JoVE58466R2
Full Title:	Optimization, test and diagnostics of miniaturized Hall thrusters
Section/Category:	JoVE Engineering
Keywords:	Space Propulsion; plasma; Thruster; Plasma acceleration; Discharge; Technology
Corresponding Author:	Igor Levchenko, Ph.D. Nanyang Technological University and Queensland University of Technology Singapore, SINGAPORE SINGAPORE
Corresponding Author's Institution:	Nanyang Technological University and Queensland University of Technology
Corresponding Author E-Mail:	igor.levchenko@qut.edu.au;I.Levchenko@post.com;levchenko.igor@nie.edu.sg
Order of Authors:	Igor Levchenko, Ph.D.
Additional Information:	
Question	**Response**
Please indicate whether this article will be Standard Access or Open Access.	Standard Access (US$1200)

Powered by Editorial Manager® and ProduXion Manager® from Aries Systems Corporation

Manuscript Click here to access/download;Manuscript;58466_R2_RE.docx

TITLE:

Optimization, Test and Diagnostics of Miniaturized Hall Thrusters

AUTHORS:

J. W. M. Lim[1], I. Levchenko[1,2], M. W. A. B. Rohaizat[1], S. Huang[1], L. Xu[1], Y. F. Sun[1], G. C. Potrivitu[1], J. S. Yee[1], R. Z. W. Sim[1], Y. M. Wang[3], S. Levchenko[1], K. Bazaka[2,1] and S. Xu[1]

[1]Plasma Sources and Applications Centre, National Institute of Education, Nanyang Technological University, Singapore

[2]School of Chemistry, Physics, Mechanical Engineering, Queensland University of Technology, Brisbane, Queensland 4000, Australia

[3]Department of Physics, School of Science, Hangzhou Dianzi University, Hangzhou 310018, China

Corresponding Author:

I. Levchenko (levchenko.igor@nie.edu.sg; Igor.Levchenko@qut.edu.au)

Email Address of Co-authors:

lim_jian_wei_mark@moe.edu.sg (J.W.M.Lim),
Muhammad255@e.ntu.edu.sg (M.W.A.B.Rohaizat),
shiyong.huang@nie.edu.sg (S. Huang),
luxiang.xu@nie.edu.sg (L. Xu),
NIE17suny6686@e.ntu.edu.sg (Y.F.Sun),
geopotrivitu@gmail.com (G. C. Potrivitu),
yee_jen_siong@moe.edu.sg (J. S. Yee),
roysmond_sim_zhen_wei@g.nie.edu.sg (R. Z. W. Sim),
ymwang0618@163.com (Y. M. Wang),
S.Levchenko@post.com (S. Levchenko),
kateryna.bazaka@qut.edu.au (K. Bazaka),
shuyan.xu@nie.edu.sg (S. Xu).

Keywords:

Electric propulsion, testing, Hall thrusters, space technology, discharge, technology

SUMMARY:

Here, we present a protocol to test and optimize space propulsion systems based on miniaturized Hall-type thrusters.

ABSTRACT:

Miniaturized spacecraft and satellites require smart, highly efficient and durable low-thrust thrusters, capable of extended, reliable operation without attendance and adjustment. Thermochemical thrusters which utilize thermodynamic properties of gases as a means of acceleration have physical limitations on their exhaust gas velocity, resulting in low efficiency. Moreover, these engines demonstrate extremely low efficiency at small thrusts and may be

unsuitable for continuously operating systems which provide real-time adaptive control of the spacecraft orientation, velocity and position. In contrast, electric propulsion systems which use electromagnetic fields to accelerate ionized gases (i.e., plasmas) do not have any physical limitation in terms of exhaust velocity, allowing virtually any mass efficiency and specific impulse. Low-thrust Hall thrusters have a lifetime of several thousand hours. Their discharge voltage ranges between 100 and 300 V, operating at a nominal power of <1 kW. They vary from 20 to 100 mm in size. Large Hall thrusters can provide fractions of millinewton of thrust. Over the past few decades, there has been an increasing interest in small mass, low power, and high efficiency propulsion systems to drive satellites of 50–200 kg. In this work, we will demonstrate how to build, test, and optimize a small (30 mm) Hall thruster capable of propelling a small satellite weighing about 50 kg. We will show the thruster operating in a large space environment simulator, and describe how thrust is measured and electric parameters, including plasma characteristics, are collected and processed to assess key thruster parameters. We will also demonstrate how the thruster is optimized to make it one of the most efficient small thrusters ever built. We will also address challenges and opportunities presented by new thruster materials.

INTRODUCTION:

Renewed interest in the space industry has in part been catalyzed by highly efficient electric propulsion systems that deliver enhanced mission capabilities at increasingly reduced launch costs[1,2,3]. Many different types of space electric propulsion devices have recently been proposed and tested[4,5,6,7,8] supported by the present-day interest in space exploration[9,10]. Among them, gridded ion[11,12] and Hall-type thrusters[13,14] are of primary interest due to their ability to reach very high efficiency of about 80%, exceeding that of any chemical thruster, including the most efficient oxygen-hydrogen systems, the efficiency of which is limited to about 5000 m/s by the principal physical laws[15,16,17,18].

Comprehensive, reliable testing of miniaturized space thrusters typically requires a large complex of test facilities that include test chambers, vacuum facilities (pumps), control and diagnostics instruments, a system for measurement of plasma parameters[19], and a wide range of auxiliary equipment that sustain the operation of the thruster, such as an electric power supply system, propellant supply unit, thrust measurement stand and many others[20,21]. Moreover, a typical space propulsion thruster consists of several units which separately influence the efficiency and service life of the whole thrust system, and therefore, could be tested both separately and as part of the thruster assembly[22,23]. This significantly complicates test procedures and implies long test periods[24,25]. Reliability of a thruster's cathode unit, as well as operation of thrusters when different propellants are used also requires special consideration[26,27].

To quantify performance of an electric propulsion system, and to qualify modules for operational deployment in space missions, ground testing facilities which enable simulation of realistic space environments are needed for testing of multi-scaled propulsion units[28,29,30]. An example of such a system is a large scaled space environment simulation chamber located at the Space Propulsion Centre–Singapore (SPC-S, **Figure 1a,b**)[31]. When developing such a simulation environment, the following primary and secondary considerations need to be taken into account. Primary concerns

are that the thus-created space environment must accurately and reliably simulate a realistic space environment, and the in-built diagnostic systems must provide precise and accurate diagnostics during performance evaluation of a system. Secondary concerns are that the simulated space environments must be highly customizable to enable rapid installation and testing of different propulsion and diagnostic modules, and the environment must be able to accommodate high throughput testing to optimize discharge and operational conditions of multiple units simultaneously.

Space environment simulators and pumping facilities

Here, we illustrate two simulation facilities at SPC-S that have been implemented for the testing of miniaturized electric propulsion systems, as well as integrated modules. These two facilities are of different scales, and primarily have different roles in the process of performance evaluation, as outlined below.

Large plasma space actuation chamber (PSAC)

The PSAC has dimensions of 4.75 m (Length) x 2.3 m (Diameter) and has a vacuum pumping suite which comprises of numerous high capacity pumps working in tandem. It is able to achieve a base pressure lower than 10^{-6} Pa. It has an integrated vacuum control readout and pump activation/purge system for evacuation and purging of the chamber. It is equipped with numerous customizable flanges, electrical feedthroughs and visual diagnostic portholes to provide line test facility. This, together with a full-suite of diagnostics capabilities mounted internally, allows it to be rapidly modified for multi-modal diagnostics. The scale of PSAC also allows for testing of completely integrated modules for applications in a simulated environment.

PSAC is the SPC-S flagship space environment simulation facility (**Figure 1c,d**). Its sheer size allows for testing of complete modules of up to a few U's mounted on a quadfilar stage. The advantage of this method would be in the real-time visualization of how the propulsion modules as mounted on different payloads may influence in situ maneuvering of payloads in space. This is simulated through the mounting and suspension of the entire payload on a proprietary quadfilar thrust measurement platform. The thruster can then be fired, and the suspended platform with the thruster and payload would be tested according to space conditions. Propellant gas feedstocks which enter the test environment via the electric propulsion modules are pumped out efficiently by the vacuum suite to ensure that the chamber's overall pressure is not altered, thus, maintaining a realistic space environment[32,33,34]. Furthermore, electric propulsion systems typically involve the production of plasmas and exploit the manipulation of trajectories of charged particles exiting the system in order to generate thrust[35]. In smaller simulation environments, the buildup of charge or plasma sheaths on the wall may affect the discharge performance through plasma-wall interactions due to its proximity to the propulsion system, especially for micropropulsion where typical thrust values are in the order of millinewtons. Therefore, special attention and emphasis must be made to account for and marginalize contributions from such factors[36]. The PSAC's large size minimizes plasma-wall interactions, rendering them negligible, giving a more accurate representation of discharge parameters and enabling monitoring of plume profiles in electric propulsion modules. The PSAC is typically used

in full module evaluation and systems integration/optimization processes which allows for quick translation of thruster prototypes into operationally ready systems for ground testing in preparation for space qualification.

Scaled plasma space environment simulator (PSEC)

The PSEC has dimensions of 65 cm x 40 cm x 100 cm and has a vacuum pumping suite which comprises of six high capacity pumps working in tandem (dry vacuum pump, turbomolecular and cryo vacuum pumps). It is able to achieve a base pressure lower than 10^{-5} Pa when the whole pumping system is operating (all pumps are in use). Pressure and propellant flows are monitored in real-time through integrated mass flow readout boxes and pressure gauges. The PSEC is primarily employed in endurance testing of thrusters. Thrusters are fired for extended periods of time to evaluate effects of plasma damage on discharge channels and on its lifetime. Additionally, as shown in **Figure 2**, a complex gas flow controller network in this facility enables quick connection of other feedstock propellants to the cathode and anodes to test compatibility of thrusters with novel propellants and effects of the latter on thruster performance. This is of increased interest to research groups working on "air-breathing" electric thrusters utilizing novel propellants during operation[37].

Integrated diagnostic facilities (multi-modal diagnostics)

Different integrated diagnostic facilities, equipped with automated integrated robotic systems (AIRS-μS)[19, 23], have been developed for the two systems in PSEC and PSAC to cater for diagnostics at different scales and purposes.

Integrated diagnostics in PSEC

The diagnostic tools in PSEC essentially hinge on real-time monitoring of discharge through extended operations. The quality management system monitors residual gas in the facility for contaminant species that arise from sputtering of material during a discharge. These trace amounts are quantitatively monitored over time to evaluate erosion rates of the discharge channel and electrodes of the thruster to estimate the thruster's lifetime. The optical emissions spectrometer (OES) complements this procedure by monitoring spectral lines corresponding to electronic transitions of contaminant species due to erosion, such as copper from the electronics. OES also enables non-invasive plasma diagnostics and active monitoring of plume profile which qualitatively evaluates performance of the thruster. Finally, a robotic Faraday probe which can be controlled remotely, or set to fully autonomous mode, is used to derive quick sweeps of the plume profile to optimize collimation of beam through parametrically varying discharge conditions (**Figure 3**).

Integrated diagnostics in PSAC

The luxury of physical space in the PSAC enables installation of multiple thruster systems at various locations due to its modular design, allowing for plug-and-play-like installation for various diagnostics simultaneously. **Figure 4** shows the internal cross-section of the PSAC in various configurations, with the fully suspended quadfilar thrust measurement platform being its most notable and permanent fixture. Turret systems, controlled autonomously or wirelessly via

Android apps using microcontrollers and Bluetooth modules, can then be mounted in a modular manner facing the thruster to obtain characteristics of the plume through the installation of various probes such as Faraday, Langmuir and Retarding Potential Analyzer (RPA). Also shown in **Figure 4** is the ability of the PSAC to allow for configurable mounting of thruster systems for rapid simultaneous diagnostics of various plasma parameters. The thrusters can be mounted vertically in a single column and tested rapidly, one after another to avoid interactions between the different thruster systems. It has been verified that efficient evaluation of up to 3 different modules at a single instance is possible, thus significantly reducing the downtime during evacuation and purging processes required otherwise when testing systems individually. On the other hand, this system is a valuable opportunity for testing the thruster assemblies that should operate in a bunch, on the same satellite. The thrusters can be mounted vertically in a single column and tested rapidly, one after another to avoid interactions between the different thruster systems. It has been tested to be effective in the evaluation of up to 3 different modules at a single instance, significantly reducing downtime during evacuation and purging processes required otherwise when testing systems individually.

It is vital to determine the thrust in micropropulsion systems accurately so that parameters such as efficiency, η_{eff} and the specific impulse I_{sp}, are accurate, thus, giving a reliable representation of the dependence of thruster performance on various input parameters such as the propellant flow, and power supplied to the different terminals of the thrusters as shown in Equations 1 and 2. Explicitly, performance evaluation of micropropulsion systems typically revolves around the measurement of thrust generated from the system at various operating parameters. Therefore, performance evaluation systems need to be calibrated according to a set of standards before being installed into the space environment for use in diagnostics and testing to ensure their reliability and accuracy[19].

$$\eta_{eff} = \frac{T^2}{2\dot{m}P} \quad (1)$$

$$I_{sp} = \frac{T}{\dot{m}g} \quad (2)$$

Typical systems employ force calibration externally before thrust measurement units are installed into the test environment[38]. However, such systems do not account for the space environments affecting the material properties of the calibration standards, and for electrical, vacuum and thermal influences on the degradation of the calibrated standards over the dynamic course of performance evaluation of the thrusters. The automated wireless calibration unit shown in **Figure 5**, on the other hand, allows for in situ calibration of the system in the simulated environment before the thruster is operational[39]. This accounts for the dynamic effects of the test environment on the measurement stage, and allows for rapid re-calibration of the system prior to firing of thrusters. The system also features a symmetric modular null thrust verification unit which verifies the thrust independently. It is operated while the thruster is operational for in situ analysis of the derived thrusts from given discharge conditions. The entire process is done via MATLAB apps, allowing users to focus on optimization of hardware and design of propulsion

systems, and expedites testing of such systems[40]. Details of this method would be elaborated in the following subsection.

PROTOCOL:

Here we present the protocols for the thrust calibration procedure and performance evaluation, independent thrust verification via null measurement and plume profilometry through spatial in situ data sensing.

1. Thrust calibration procedure and thrust performance evaluation

1.1. Ensure that all components are installed in the chamber as shown in **Figure 5**.

1.2. Test the connectivity of the diagnostic tools externally before sealing the chamber.

1.3. Use the integrated facility control to seal the chamber.

1.4. Turn on the vacuum pumps in cascading order starting from the dry pumps (until the chamber reaches 1 Pa), turbo-molecular pumps (until it reaches ~5 x 10^{-4} Pa), and then the cryogenic pumps.

NOTE: PSAC is left to pump down to high vacuum (< ~10^{-5} Pa) to simulate space environment. The protocol can be paused here.

1.5. Use the developed apps to synchronize the devices with the wireless transponder in the chamber. The synchronization process is complete when the light-emitting diode (LED) on the transponder stops flashing.

1.6. Once the desired vacuum has been obtained, take an initial reading (analog voltage) off the laser displacement sensor as a baseline.

1.7. Use the developed app to trigger the lowering of a weight (of a precisely known and calibrated mass of copper loop) for force translation on the quadfilar stage.

NOTE: The mass of each copper loop depends on the intended sensitivity of the quadfilar stage being used. In this case, the mass of each copper loop was in the order of 100 mg for the extended calibration regime and 10 mg for the fine calibration regime. See the representative results for more information.

1.8. Record the displacement (analog voltage) from the laser displacement sensor when it is triggered after the mass is fully lowered and its weight is translated into a horizontal force.

1.9. Repeat the process (steps 1.7 and 1.8) of lowering the weights and recording of the displacement of the quadfilar stage until all the calibrations weights are expanded. All the weights will be automatically returned to the equilibrium position by the calibration unit after

the sequence is completed to allow the quadfilar stage to reach an equilibrium position before thruster can be fired. Save the calibration factor (**File** | **Save as** | "Factor.txt").

1.10. Draw a calibration curve to obtain the calibration factor for the system installed on the quadfilar stage, where the calibration factor (in mN/V) is the gradient of the force/voltage graph.

1.11. Record a baseline analog voltage from the laser displacement sensor again before firing the thruster.

1.12. Activate the in situ MATLAB program for calculating thrust instantaneously using Equation 3 (see the representative results) and input the calibration factor derived in step 1.9 (**File** | **Open** | "Factor.txt").

1.13. The thrusters can then be fired again. Capture the desired parameters in real time using the in-house data acquisition program.

NOTE: Alternatively, an integrated app can be used to fully automate the calibration process while synchronizing the actuation sequence from the motors, and data acquisition from the sensors accordingly.

2. Null measurement protocol for independent thrust verification

2.1. First, take a baseline (analog voltage) reading (from the laser displacement sensor) of the thruster in equilibrium position.

2.2. Toggle operational parameters to desired values from the thruster control panel and fire the thruster.

2.3. Once the thruster is fired, wait for the oscillations on the quadfilar pendulum to stabilize.

2.4. After the quadfilar stabilizes to a steady state, use the control app for the null measurement system to trigger the lowering of weights. Readings from the laser displacement sensor are monitored simultaneously. The weights are continually lowered until the quadfilar stage is actuated back into equilibrium.

2.5. Once the equilibrium position is reached, terminate the actuation sequence, and determine the force required to bring the quadfilar system back to equilibrium.

2.6. Trigger a stopper block to stop the quadfilar stage from moving.

2.7. Compute mass corresponding to the horizontal force required to pull the system back into equilibrium.

3. Actuation of robotic turrets for spatial in situ data sensing and plume profilometry

NOTE: During operation of the thruster, an operator may choose to actuate the system manually to desired angles to obtain plume characteristics at particular locations or trigger an automated sequence.

3.1. Mount the thruster on a moving stage (as in the case of PSAC) before starting the experiment.

3.2. Activate the stop-bar mechanism to prevent the stage from actuating during the experiment.

3.3. Trigger the measurement protocol and servo motor to actuate the probe to the 0° position.

3.4. Acquire a measurement from the probe.

NOTE: Depending on the type of probes installed, the measurement processes can be varied according to the programmable sequence for obtaining complete spatial plume profiles of the discharge. (a) If a Faraday probe is mounted, a reading off a source meter is taken (where a bias of -30 V is continuously applied to the guard rings). (b) If a Langmuir probe is mounted, a sawtooth voltage waveform is supplied to the probe and the I-V characteristics are obtained and interpreted. (c) If an RPA is mounted, a sawtooth voltage waveform is applied to the discriminating grid, and the I-V characteristics are obtained and interpreted.

3.5. Trigger the servo motor using the microcontroller, to move to the next angular position where the probe sequence is triggered to make a measurement again.

3.6. Save the measurements in individually marked arrays in a data matrix.

3.7. Repeat steps 3.5 and 3.6 until a full sweep up to 180° has been performed, and the probe is brought back to 0°.

3.8. Analyze the saved data.

REPRESENTATIVE RESULTS:

Thrust calibration procedure and thrust performance evaluation

Evaluation of thrust values from the quadfilar thrust measurement stage comes in two phases. The first phase is through obtaining calibration factors from the automated wireless calibration unit shown to the right of **Figure 5**. In this calibration process, fine weights are lowered across a smooth polytetrafluoroethylene bar which translates the vertical effects of a weight into a horizontal force as attached to the thruster on the quadfilar stage. A high-resolution laser displacement sensor then measures the displacement at each interval accordingly. This is monitored by an operator via a data acquisition app as shown in **Figure 6,** and a calibration factor is obtained at the end of the series where numerous calibrated weights are lowered onto the

system. The calibration factor S is obtained from the best fit line of the horizontal force-displacement graph, and the subsequent thrust is calculated using Equation 3:

$$T = (V_{baseline} - V_{measured})S \quad (3)$$

where $V_{baseline}$ is the analog baseline voltage from the laser displacement sensor read prior to firing the thruster, and $V_{measured}$ is the measured voltage from the sensor during in situ operation of the thruster.

A clearer representation of the calibration system is shown in **Figure 7**. It is to be noted that the green line and red circles are for illustration purposes only and merely serve as a guide for the eye. In reality, the green line is a fine Madeira polyamide fiber which connects to the mounted thruster. The calibrated weights are small copper loops that have been carefully weighed by a high precision mass balance, and they can be adjusted accordingly to allow for a fine calibration regime initially (with smaller intervals in difference between masses), and to an extended regime (where larger masses are added towards the end of the calibration sequence).

A typical force-voltage graph will produce a straight line as shown in **Figure 8** when the calibration unit, laser displacement sensor and quadfilar platform are properly installed. In this case, the plot yields a calibration factor (gradient) of 27.65 $mN \cdot V^{-1}$ in a standardized set up for thrust measurements over a wide range of forces.

The calibration factor can be altered by modifying the sensitivity of the quadfilar platform, which depends on several factors such as the length of the quadfilar wires. In **Figure 8**, the sensitivity of the setup has been modified to fit in calibration weights for extended regimes. Both fine and coarse calibration weights are included to yield a calibration plot that is linear in both regimes.
A sample of the in situ measurements for thrust measured is shown in **Figure 9**. In this case, it shows how an operator is able to monitor the dependence of thrust on discharge voltage during the course of the experiment until the discharge is extinguished. Effects of other input parameters on the thrust can also be monitored in the same manner.

Using the quadfilar thrust measurement stage, we were able to measure the thrust generated by our hall thruster at various input powers, given by the discharge current and applied voltage. Through this information, the variation of η_{eff} and I_{sp} with respect to input power can be obtained. **Figure 10a,b** shows how the thrust and I_{sp} vary with input power at 4 different mass flow rates. Finally, the efficiency is plotted against the input power at different mass flow rates in **Figure 10c**. The results show that our thruster has been optimized to work at input powers below 100 W, where low flow rates have resulted in efficiencies of almost 30%[19]. Prior to optimization, the thruster barely achieved 20% efficiency at 83 W and 5.5 sccm. The results show that our thruster has been optimized to work at input powers below 100 W, where low flow rates have resulted in efficiencies of almost 30%[19]. This is arguably a decent achievement compared to the SPT100 Hall thruster, whose efficiency varies between 30% to 40%, and other Hall thrusters of similar sizes and input powers[41,42]. **Figure 10d** illustrates the automatically plotted profile of ion current density.

Null measurement protocol for independent thrust verification

While the thruster is being fired, the polyamide wire on the right-hand side corresponding to the calibration unit end is left slack. During the in situ operation of the thruster, the symmetric null measurement verification unit can then be triggered. The symmetric null measurement unit operates in a similar manner to the robotic calibration system shown in **Figure 5**; the miniature calibration weights attached to a fine polyamide wire are lowered in the system and create a horizontal force applied to the propulsion system. In this case, the horizontal force is applied to pull the quadfilar system which has been displaced upon operation of the thruster back to equilibrium. This process is shown in the time-dependent schematic of the process evolution in **Figure 11**. The thruster is first fired at t = 0 s, corresponding to panel (a) in the series. The quadfilar stage then displaces to the right as a result of the horizontal force from the propulsion unit. Since the environment is darkened in the space simulator, the motion of the stage is seen as the apparent movement of the thruster in (b). The quadfilar stage then stops oscillating and reaches an equilibrium steady state displacement as shown in (c). At this instance, the null system is triggered and the stepper motor is activated to pull the quadfilar stage back to equilibrium as shown in (d). The stepper motor is triggered to a point where the laser displacement sensor detects that the stage is back in the equilibrium position and the actuation is stopped. A measurement is then taken, and the thrust value from this system is given accordingly.

Actuation of robotic turrets for spatial in situ data sensing and plume profilometry

Modular robotic turret systems are also installed in both PSAC and PSEC for customizable diagnostics of plume profiles. These robotic turrets are also mounted on motor actuated stages for proper probe positioning according to the axial centerline of the thrusters externally. The robotic turrets comprise of shielded stainless steel enclosures containing programmable microcontrollers attached to wireless transponders for receiving and transmitting data. This also allows users to control the movement of the probe externally, while receiving data from sensors without additional electrical connections to the system. It is also worth noting that the modular design of the micro-servo motor actuated turret allows quick refinement of measurement setup that allows for multiple probe arrays including Langmuir, Faraday probe and RPAs be mounted on the same set up according to operational demands at the point of time. **Figure 12** shows a schematic illustration of the experimental setup for plume profilometry.

During operation of the thruster, an operator can choose to manually actuate the system to desired angles as illustrated in **Figure 12** to obtain plume characteristics at particular locations, or an automated sequence can be triggered. Depending on which probes are installed, the measurement processes can be varied according to the programmable sequence for obtaining complete spatial plume profiles of the discharge.

Such a sequence allows for quick spatial visualization of the plume profile which helps optimize engineering and process optimization in allowing for beam collimation for efficient thruster operation. Actuated turrets and programmable sensing systems allow for autonomous

acquisition of plume characteristics at each point, where plasma parameters may be derived and calculated through programmable systems. This may expedite testing of such systems with easy analysis and manipulation of large amounts of data through simple robotic and actuated autonomous systems. In **Figure 10d,** for example, the plasma parameter being analyzed here is the ion current density at different angular positions. It shows how the discharge power influences the magnitude of the peak ion current density and the full-width at half maxima accordingly. These results show that higher discharge voltages do not necessarily translate to better thruster performance. Here, higher power results in the widening of the plume profile which is an undesirable characteristic of a thruster. This means that some of the exhaust particles have velocities which are not perpendicular to the thruster exit plane, resulting in a thrust in an unintended direction and making precise maneuvers challenging. Moreover, the charges from the plume may damage the payload or other subsystems on the spacecraft[43]. To optimize the thruster to produce a more collimated plume, the current supplied to the magnetic coils and the potential drop at the anode can be adjusted until a satisfactory full-width at half maxima (FWHM) value has been achieved. Prior to plume profile optimization, its FWHM was 33.1° at 140 W but after optimization, it reduced to 23.7° at 110 W. This implies that the plume is now more collimated.

FIGURE LEGENDS:

Figure 1: Large space environment facility for testing of electric propulsion thrusters. This flagship facility is located at the Space Propulsion Centre Singapore, National Institute of Education, Nanyang Technological University. (**a**) Side view of the chamber illustrates transparent portholes for visual diagnostics of test systems, and the multiple vacuum grade electrical feed-throughs that allow for communication, control and diagnostics of systems under test. (**b**) Vacuum pumps. (**c**) Side view of the chamber with a side loading hatch open. (**d**) View of the space simulation chamber with an operator installing diagnostic systems.

Figure 2: Rear view of a scaled plasma space environment simulator (PSEC). PSEC comprises a total of 6 pumps including high capacity cryogenic pumps, turbo-molecular pumps, and dry pumps. The setup also contains integrated thruster diagnostics.

Figure 3: Overview of a plasma diagnostics suite in the PSEC. Right hand side of the figure illustrates a magnified view of the systems as viewed from the porthole from the front of the chamber. The visual diagnostic port also serves as an avenue for optical emission spectroscopy (OES) to be done. As shown in the exterior view of the chamber, a quadropole mass spectrometer is outfitted for residual gas analysis to evaluate material erosion rates due to sputtering in the chamber during prolonged thruster operation. Additionally, wirelessly controlled robotic Faraday probes are also mounted internally to evaluate plume profiles of the thrusters undergoing performance evaluation.

Figure 4: Overview of the integrated plasma diagnostics suite in the PSAC. (**a**) Customizable design shows a robotic Faraday probe turret placed alongside a quadfilar thrust performance evaluation stage, and an in-situ weight calibration unit. (**b**) Customizable features allow for up to

three different thrusters to be mounted and tested simultaneously, reducing operational downtime and maximizing research output.

Figure 5: Schematic layout of the symmetric modular null thrust verification unit. Unlike the calibration system, the null thrust verification unit is operated while the thruster is fired to allow for independent verification of the thrust values obtained.

Figure 6: Data acquisition app user interface. The user interface of the MATLAB-based app allows the operator to monitor the thrust and voltage reading from the laser displacement sensor in real time.

Figure 7: Calibration unit. A robotic calibration unit can be operated by a wireless operator input, or through fully autonomous calibration sequences for quick calibration of a quadfilar system. Design considerations: Minimize external influence; use thin, light weight string and millinewton weights; use low static coefficient bar; line must be flexible enough to produce "u-loop". For the calibration stand, use wireless control unit, fine Madeira monofilament polyamide (nylon) fiber (about 4.0 µm), small copper loops as weights and a smooth polytetrafluoroethylene bar. Line should be attached to rear of mounted thruster on quadfilar pendulum or in line with the center of the reflector plate.

Figure 8: Typical force-voltage and force-voltage graphs for modified setup. (**a**) Force-voltage graph. The amount of weight which has been lowered and translated into a horizontal force is plotted against the corresponding voltage reading on the laser displacement sensor. The calibration factor (in mN/V) is the gradient of the force/voltage graph which will be used in the data acquisition app. (**b**) Force/voltage graph. The sensitivity of the setup towards the applied force was increased to accommodate for both fine and coarse calibration.

Figure 9: In-situ performance evaluation. Another software program allows the thrust performance to be monitored in real-time when an input parameter, the discharge voltage in this case, is changed gradually.

Figure 10: Evaluation of thruster characteristics. (**a**, **b**) Thrust and specific pulse as functions of input power at four different mass flow rates. (**c**) Efficiency plotted against the input power at different mass flow rates. (**d**) The automatically plotted profile of ion current density.

Figure 11: Time evolution of the null thrust verification unit in operation during firing of a Hall thruster at SPC-S. (**a**) t = 0 s, where the Hall thruster is first fired and moves away from the equilibrium position. (**b**) Quadfilar stage displaces to the right as shown by the relative motion of the Hall thruster. (**c**) Quadfilar stage stops oscillating and reaches an equilibrium steady-state position. Null system is triggered and the stepper motor actuation commences. (**d**) Null system is triggered to slowly pull the thruster mounted on the quadfilar stage back to equilibrium. (**e**) Thruster reaches an equilibrium position. Null measurement unit stops the stepper motor actuation. Measurement is taken.

Figure 12: Schematic representation of the actuation of the modular multi-probe turret. The entire system is controlled wirelessly, and Faraday probe can be replaced quickly through snapping on a different probe module. Connections are made through BNC-type adapters for easy twist-on conversion and installation.

Figure 13: Schematics of a Hall-type thruster. Similar setups with varied configurations based on a generalized layout presented in this figure have also been employed by other groups.

Figure 14: Inductively Coupled Plasma Facility for synthesis of novel materials at the Plasma Sources Application Centre / Space Propulsion Centre, Singapore. A powerful plasma system enables synthesis of silicon-based materials for innovative, highly efficient solar cells, as well as boron nitride and other nanostructured materials for applications in the modern miniaturized thrusters.

DISCUSSION:

Typical Hall-type thrusters[44] are relatively simple, cheap and highly efficient devices that could accelerate an ion flux to the velocities of several tens of km/s, providing thrust required for accelerating satellites and spacecraft, as well as for maneuvering, orientation, position and attitude control, and de-orbiting at the end of their operation service life. Application of Hall thrusters on satellites and other orbital payloads enhance mission lifetime, allow orbital transfer and formation/constellation flying of multiple satellites, and enable multi-mission capabilities. Structurally (see schematics in **Figure 13**), a Hall thruster is a coaxial chamber with an anode installed at one side, and a cathode placed near the exit. Easily ionized but relatively heavy, Xe gas, is usually used as a propellant, yet other elements such as iodine could be used in some cases[45]. An ion flux is accelerated by an electrostatic field that is set between the anode and cathode, while a magnetic field created by a set of coils or a system of permanent magnets ensures an electron drift current around the central part of the chamber[46]. This electron drift current ensures efficient ionization of a neutral gas and simultaneously, it provides compensation of a positive ion change.

The efficiency of an electric propulsion thruster depends significantly on its design, especially the shape and configuration of electrodes and parameters of the magnetic field, and materials used for the accelerating channel, anode and emissive inserts in the cathode. For example, the magnetic field topology of the thruster can be configured in such a way that the location of maximum magnetic field strength and hence, the ionization zone are pushed further downstream, near the channel outlet, thus, reducing the interaction between high energy ions and the channel wall[47]. This in turn reduces erosion rates of the channel wall and its dependence on wall material properties, making wall material replacement more feasible. The lifetime of Hall-type thrusters depends highly upon the materials used for its components, especially the ones that are in contact with the plasma. Going forward, novel materials, as well as equipment and techniques for its synthesis and testing[48,49] are needed to further improve the lifetime of Hall-type thrusters.

Novel materials are synthesized in the PSAC/SPCS labs using mainly a powerful, highly adaptive, efficient inductively coupled plasma facility (**Figure 14**)[50,51]. A spectrum of novel materials includes, but is not limited to silicon-based wafers for innovative, highly efficient solar cells, as well as boron nitride, graphene-containing nanostructures[52,53], metamaterials[54,55] and other nanostructured materials for applications in modern miniaturized thrusters, where they are used for significant intensification and optimization of the key parameters of thrusters[56,57]. Other available equipment include arc and capacitive-coupled plasma systems for the for advanced plasma treatment of materials[58]. Indeed, a significant enhancement of thruster parameters could be attained through implementation of sophisticated test, design, materials and simulation optimization techniques[59,60]. Moreover, applications of novel materials and material systems could ensure efficient approaches towards, e.g., heat transfer[61], wear resistance[62], and other problems associated with the efficiency and service life of miniaturized space thrusters. Plasma-based material facilities enable synthesis, test and application of the most advanced materials in the thrusters currently being designed[63]. Indeed, it has already been demonstrated that plasma-enabled techniques which involve highly energetic fluxes on matter and energy, allow for efficient activation of surfaces[64,65] and hence, control over self-organization, nucleation[66,67,68] and other sophisticated surface-based processes leading to the creation of the most advanced materials[69,70,71]. Note that carbon-containing materials such as carbon nanowalls, nanotubes and vertically-oriented graphene arrays could be quite promising for the application in the electric propulsion thrusters as electron emitting materials[72,73,74] and promising material for the walls of acceleration channels and discharge chambers[75].

Plasma-made multilayered, core-shell and porous materials[76] could also find applications in various parts of the electric propulsion systems[77]. Controlled synthesis of metallic single-walled carbon nanotubes[78] and plasma-enabled, catalyst-free growth of carbon nanotubes on mechanically-written Si features[79] is also possible in the plasma-driven process[80].

In summary, we have presented a protocol to test and optimize miniaturized space propulsion systems. Diversified sophisticatedly designed equipment, large vacuum chambers, powerful pumping platforms and various diagnostic complexes were used to perform precise, informative characterization of micro-propulsion thrusters under conditions close to those found in open space. Skilled personnel, adequate simulation and theoretical support are also of key importance to keep the micropropulsion design and technology progressing steadily. Development of novel materials is the second key factor that could ensure significant breakthroughs in improving performance characteristics of modern electric propulsion systems, including small satellites and CubeSats with the whole set of supply systems, peripheral instruments, tools and payload.

ACKNOWLEDGEMENTS:

This work was supported in part by OSTIn-SRP/EDB, the National Research Foundation (Singapore), Academic Research Fund AcRF Tier 1 RP 6/16 (Singapore), and the George Washington Institute for Nanotechnology (USA). I. L. acknowledges the support from the School of Chemistry, Physics and Mechanical Engineering, Science and Engineering Faculty, Queensland University of Technology.

DISCLOSURES:

The authors declare no competing financial or other interests.

REFERENCES:

1. Levchenko, I., Keidar, M., Cantrell, J., Wu, Y.-L., Kuninaka, H., Bazaka K., Xu, S. Explore space using swarms of tiny satellites. *Nature* **562**, 185-187 (2018).
2. Kishi, N. Management analysis for the space industry. *Space Policy* **39–40**, 1-6 (2017).
3. Chen, Y. China's space policy-a historical review. *Space Policy* **37**, 171-178 (2016).
4. Levchenko, I., Bazaka, K., Mazouffre, S., and Xu, S. Prospects and physical mechanisms for photonic space propulsion. *Nature Photonics* **12**, 649–657 (2018).
5. Mazouffre, S. Electric propulsion for satellites and spacecraft: established technologies and novel approaches. *Plasma Sources Sciency and Technology* **25**, 033002 (2016).
6. Rafalskyi, D., Aanesland, A. Brief review on plasma propulsion with neutralizer-free systems. *Plasma Sources Sciency and Technology* **25**, 043001 (2016).
7. Levchenko, I., Bazaka, K., Ding, Y., Raitses, Y., Mazouffre, S., Henning, T., Klar, P. J. *et al*. Space micropropulsion systems for Cubesats and small satellites: from proximate targets to furthermost frontiers. *Applied Physics Reviews* **5**, 011104 (2018).
8. Garrigues, L., Coche, P. Electric propulsion: comparisons between different concepts. *Plasma Physics and Controlled Fusion* **53**, 124011 (2011).
9. Levchenko, I., Xu, S., Mazouffre, S., Keidar, M., Bazaka, K. Mars Colonization: Beyond Getting There. *Global Challenges* **2**, 1800062 (2018).
10. Grimaud, L., Mazouffre, S. Performance comparison between standard and magnetically shielded 200 W Hall thrusters with BN-SiO2 and graphite channel walls. *Vacuum* **155**, 514-523 (2018).
11. Choueiri, E. Y. A critical history of electric propulsion: the first 50 years (1906-1956). *Journal of Propulsion and Power* **20**, 193-203 (2004).
12. Ozaki, T., Kasai, Y., Nakagawa, T., Itoh, T., Kajiwara, K., Ikeda, M. In-Orbit Operation of 20 mN Class Xenon Ion Engine for ETS-VIII. 28th International Electric Propulsion Conference, IEPC-2007-084, Florence, Italy, September 17–20 (2007).
13. Ding, Y., Li, H., Li, P., Jia, B., Wei, L., Su, H., Sun, H., Wang, L., Yu, D. Effect of relative position between cathode and magnetic separatrix on the discharge characteristic of hall thrusters. *Vacuum* **154**, 167-173 (2018).
14. Ding, Y., Peng, W., Sun, H., Wei, L., Zeng, M., Wang, F., Yu, D. Performance characteristics of No-Wall-Losses Hall thruster. *The European Physical Journal - Special Topics* **226**, 2945-2953 (2017).
15. Ahedo, E. Plasmas for space propulsion. *Plasma Physics and Controlled Fusion* **53**, 124037 (2011).
16. Charles, C. Plasmas for spacecraft propulsion. *Journal of Physics D: Applied Physics* **42**, 163001 (2009).
17. Ding, Y., Sun, H., Li, P., Wei, L., Su, H., Peng, W., Li, H., Yu, D. Application of hollow anode in Hall thruster with double-peak magnetic fields. *Journal of Physics D: Applied Physics* **50**, 335201 (2017).

18. Conversano, R. W., Goebel, D. M., Mikellides, I. G., Hofer, R. R. Performance analysis of a low-power magnetically shielded Hall thruster: computational modeling. *Journal of Propulsion and Power* **33**, 992-1001 (2017).
19. Chen, F. F. Langmuir probe analysis for high density plasmas. *Physics of Plasmas* **8**, 3029-3041 (2001).
20. Neumann, A. Update on diagnostics for DLR's electric propulsion test facility. *Procceedins of Engineering* **185**, 47-52 (2017).
21. Snyder, J. S., Baldwin, J., Frieman, J. D., Walker, M. L., Hicks, N. S., Polzin, K. A., Singleton, J. T. Recommended practice for flow control and measurement in electric propulsion testing. *Journnal of Propulsion and Power* **33**, 556-565 (2017).
22. Conversano, R. W., Goebel, D. M., R. R. Hofer, I. G. Mikellides, R. E. Wirz. Performance analysis of a low-power magnetically shielded hall thruster: Experiments. *Journal of Propulsion and Power* **33**, 975-983 (2017).
23. Pottinger, S., Lappas, V., Charles, C., Boswell, R. Performance characterization of a helicon double layer thruster using direct thrust measurements. *Journal of Physics D: Applied Physics* **44**, 235201 (2011).
24. Ding, Y., Peng, W., Sun, H., Wei, L., Zeng, M., Wang, F., Yu, D. Visual evidence of suppressing the ion and electron energy loss on the wall in Hall thrusters. *Japanese Journal of Applied Physics* **56**, 038001 (2017).
25. Ding, Y., Peng, W., Wei, L., Sun, G., Li, H., Yu, D. Computer simulations of Hall thrusters without wall losses designed using two permanent magnetic rings. *Journal of Physics D: Applied Physics* **49**, 465001 (2016).
26. Rovey, J. L., Gallimore, A. D. Dormant cathode erosion in a multiple-cathode gridded ion thruster. *Journal of Propulsion and Power* **24**, 1361-1368 (2008).
27. Linnell, J. A., Gallimore, A. D. Efficiency analysis of a hall thruster operating with krypton and xenon. *Journnal of Propulsion and Power* **22**, 1402-1412 (2006).
28. Funaki, I., Iihara, S., Cho, S., Kubota, K., Watanabe, H., Fuchigami, K., Tashiro, Y. Laboratory Testing of Hall Thrusters for All-electric Propulsion Satellite and Deep Space Explorers. *52nd AIAA/SAE/ASEE Joint Prop. Conf., AIAA Propulsion and Energy Forum (AIAA 2016-4942)*.
29. Ding, Y., Sun, H., Li, P., Wei, L., Xu, Y., Peng, W., Su, H., D, Yu. Influence of hollow anode position on the performance of a Hall-effect thruster with double-peak magnetic field. *Vacuum* **143**, 251-261 (2017).
30. Ding, Y., Peng, W., Sun, H., Xu, Y., Wei, L., Li, H., Zeng, M., Wang, F., Yu, D. Effect of oblique channel on discharge characteristics of 200-W Hall thruster. *Physics of Plasmas* **24**, 023507 (2017).
31. Lim, J. W. M., Huang, S. Y., Xu, L., Yee, J. S., Sim, R. Z., Zhang, Z. L., Levchenko, I., Xu, S. Automated Integrated robotic systems for diagnostics and test of electric and μ-propulsion thrusters. *IEEE Transaction of Plasma Sciency* **46**, 345-353 (2018).
32. Underwood, C., Sergio, P., Lappas, V. J., Bridges, C. P., Baker, J. Using CubeSat/micro-satellite technology to demonstrate the autonomous assembly of a reconfigurable space telescope (AAReST). *Acta Atronaut.* **114**, 112-122 (2015).

33. Kamahawi, H., Huang, W., Haag, T. Investigation of the effects of facility background pressure on the performance and voltage-current characteristics of the high voltage hall accelerator. AIAA, 2014.
34. Lim, J. W. M., Huang, S. Y., Sun, Y. F., Xu, L., Sim, R. Z. W., Yee, J. S., Zhang, Z. L., Levchenko, I., Xu, S. Precise calibration of propellant flow for practical applications and testing in Hall thruster setups. *IEEE Transaction on Plasma Science* **46**, 338-344 (2018).
35. Boeuf, J. P. Tutorial: Physics and modeling of Hall thrusters. *Journal of Applied Physics* **121**, 011101 (2017).
36. Ikeda, T., Togawa, K., Tahara, H., Watanabe, Y. Performance characteristics of very low power cylindrical Hall thrusters for the nanosatellite 'PROITERES-3'. *Vacuum* **88**, 63-69 (2013).
37. Jackson, S. W., Marshall, R. Conceptual design of an air-breathing electric thruster for CubeSat applications. *J. Spacecraft Rockets,* In press, 2017.
38. Rohaizat, M. W. A. B., Lim, M., Xu, L., Huang, S., Levchenko, I., Xu, S. Development and calibration of a variable range stand for testing space micropropulsion thrusters. *IEEE Transaction on Plasma Science* **46**, 289-295 (2018).
39. Raitses, Y., Fisch, N. J. Parametric investigations of a nonconventional Hall thruster. *Physics of Plasmas* **5**, 2579 (2001).
40. Vaudolon, J., Mazouffre, S., Henaux, C., Harribey, D., Rossi, A. Optimization of a wall-less Hall thruster. *Applied Physics Letters* **107**, 174103 (2015).
41. Mazouffre, S., Grimaud, L. Characteristics and Performances of a 100-W Hall Thruster for Microspacecraft. *IEEE Transactions on Plasma Science* **46**, 330-337 (2018).
42. Levchenko, I. *et al.* Recent progress and perspectives of space electric propulsion systems based on smart nanomaterials. *Nature Communications.* **9**, 879, (2018).
43. Goebel, D. M., Katz, I. *Fundamentals of electric propulsion*. (Wiley, 2008).
44. Choueiri, E. Y. Fundamental difference between the two Hall thruster variants. *Physics of Plasmas* **8**, 5025 (2001).
45. Ding, Y., Sun, H., Peng, W., Xu, Y., Wei, L., Li, H., Li, P., Su, H., Yu, D. Experimental test of 200 W Hall thruster with titanium wall. *Journal of Physics D: Applied Physics* **56**, 050312 (2017).
46. Lemmer, K. Propulsion for CubeSats. *Acta Astronautics* **134**, 231-243 (2017).
47. Ding, Y. *et al.* A 200-W permanent magnet Hall thruster discharge with graphite channel wall. *Physics Letters A.* **382** (42), 3079-3082, (2018).
48. Levchenko, I., Bazaka, K., Belmonte, T., Keidar, M., Xu, S. Advanced Materials for Next Generation Spacecraft. *Advanced Materials* **30**, 1802201 (2018).
49. M. V. Jacob, R. S. Rawat, B.Ouyang, K.Bazaka, D. S. Kumar, D. Taguchi, M. Iwamoto, R. Neupane, O. K. Varghese. Catalyst-Free Plasma Enhanced Growth of Graphene from Sustainable Sources. *Nano Letters* **15**, 5702-5708 (2015).
50. Baranov, O., Bazaka, K., Kersten, H., Keidar, M., Cvelbar, U., Xu, S., Levchenko, I. Plasma under control: Advanced solutions and perspectives for plasma flux management in material treatment and nanosynthesis. *Applied Physics Reviews* **4**, 041302 (2017).

51. Levchenko, I., Bazaka, K., Baranov, O., Sankaran, M., Nomine, A., Belmonte, T., Xu, S. Lightning under water: Diverse reactive environments and evidence of synergistic effects for material treatment and activation. *Applied Physics Reviews* **5**, 021103 (2018).
52. Bazaka, K., Jacob, M. V., Ostrikov, K. Sustainable Life Cycles of Natural-Precursor-Derived Nanocarbons. *Chemical Reviews* **116**, 163–214 (2016).
53. Levchenko, I., Ostrikov, K. K., Zheng, J., Li, X., Keidar, M., K. B. K. Teo. Scalable graphene production: perspectives and challenges of plasma applications. *Nanoscale* **8**, 10511 (2016).
54. Levchenko, I., Bazaka, K., Keidar, M., Xu, S., Fang, J. Hierarchical Multi-Component Inorganic Metamaterials: Intrinsically Driven Self-Assembly at Nanoscale. *Advanced Materials* **30**, 1702226 (2018).
55. Baranov, O., Levchenko, I., Bell, J. M., Lim, J. W. M., Huang, S., Xu, L., Wang, B., Aussems, D. U. B., Xu, S., Bazaka, K., From nanometre to millimetre: a range of capabilities for plasma-enabled surface functionalization and nanostructuring. *Materials Horizons* **5**, 765-798 (2018).
56. Koizumi, H. , Kuninaka, H. Miniature Microwave Discharge Ion Thruster Driven by 1 Watt Microwave Power. *Journal of Propulsion and Power* **26**, 601-604 (2010).
57. Ding, Y., Su, H., Li, P., Wei, L., Li, H., Peng, W., Xu, Y., Sun, H., Yu, D. Study of the Catastrophic Discharge Phenomenon in a Hall Thruster. *Physics Letters A* **381**, 3482-3486 (2017).
58. Baranov, O., Xu, S., Ostrikov, K., Wang, B. B., Bazaka, K., Levchenko, I. Towards universal plasma-enabled platform for the advanced nanofabrication: plasma physics level approach. *Reviews of Modern Plasma Physics* **2**, 4 (2018).
59. Taccogna, F. Monte Carlo Collision method for low temperature plasma simulation. *Journal of Plasma Physics* **81**, 305810102 (2014).
60. Furukawa, T., Takizawa, K., Kuwahara, D., Shinohara, S. Electrodeless plasma acceleration system using rotating magnetic field method featured. *AIP Advances* **7**, 115204 (2017).
61. Levchenko, I., Beilis, I. I., Keidar, M. Nanoscaled metamaterial as an advanced heat pump and cooling media. *Advanced Materials Technologies* **1**, 1600008 (2016).
62. Zidar, D. G., Rovey, J. L. Hall-Effect Thruster Channel Surface Properties Investigation. *Journal of Propulsion and Power*, **28**, 334-343 (2012).
63. Pai, D. Z., Ostrikov, K. K., Kumar, S., Lacoste, D. A., Levchenko, I. and Laux, C. O. Energy efficiency in nanoscale synthesis using nanosecond plasmas, *Scientific Reports* **3**, 1221 (2013).
64. Rider, A. E., Levchenko, I., Ostrikov, K. Surface fluxes of Si and C adatoms at initial growth stages of SiC quantum dots. *Journal of Applied Physics* **101**, 044306 (2007).
65. Bazaka, K., Baranov, O., Cvelbar, U., Podgornik, B., Wang, Y., Huang, S., Xu, L., Lim, J. W. M., Levchenko, I., Xu, S. Oxygen plasmas: a sharp chisel and handy trowel for nanofabrication. *Nanoscale* **10**, 17494-17511 (2018).
66. Levchenko, I., Ostrikov, K., Murphy, A. B. Plasma-deposited Ge nanoisland films on Si: is Stranski–Krastanow fragmentation unavoidable? *Journal of Physics D: Applied Physics* **41**, 092001 (2008).

67. Hundt, M., Sadler, P., Levchenko, I., Wolter, M., Kersten, H., Ostrikov, K. Real-time monitoring of nucleation-growth cycle of carbon nanoparticles in acetylene plasmas. *Journal of Applied Physics* **109**, 123305 (2011).
68. Levchenko, I., Cvelbar, U., Ostrikov, K. Kinetics of the initial stage of silicon surface oxidation: Deal–Grove or surface nucleation? *Applied Physics Letters* **95**, 021502 (2009).
69. Han, Z. J., Rider, A. E., Ishaq, M., Kumar, S., Kondyurin, A. *et. al*.. Carbon nanostructures for hard tissue engineering. *RSC Advances* **3**, 11058-11072 (2013).
70. Levchenko, I., Ostrikov, K. Carbon saturation of arrays of Ni catalyst nanoparticles of different size and pattern uniformity on a silicon substrate. *Nanotechnology* **19**, 335703 (2008).
71. Baranov, O., Levchenko, I., Xu, S., Lim, J. W. M., Cvelbar, U., K Bazaka. Formation of vertically oriented graphenes: what are the key drivers of growth? *2D Materials* **5**, 044002 (2019).
72. Singh, L. A., Sanborn, G. P., Turano, S. P., Walker, M. L. R. Ready, W. J. Operation of a carbon nanotube field emitter array in a Hall effect thruster plume environment. *IEEE Transactions on Plasma Science* **43**, 95 (2015).
73. Levchenko, I., Ostrikov, K. Plasma/ion-controlled metal catalyst saturation: Enabling simultaneous growth of carbon nanotube/nanocone arrays. *Applied Physics Letters* **92**, 063108 (2008).
74. Milne, W. I., Teo, K. B. K., Amaratunga, G. A. J., Legagneux, P., Gangloff, L., Schnell, J. P., Semet, V., Binh, V. T., Groening, O. Carbon nanotubes as field emission sources. *Journal of Materials Chemistry* **14**, 933 (2004).
75. Lee C., Wei X., Kysar J. W., Hone J. Measurement of the elastic properties and intrinsic strength of monolayer graphene. *Science* **320**, 385 (2008).
76. Fang, J. *et. al*. Plasma-enabled growth of single-crystalline SiC/AlSiC core–shell nanowires on porous alumina templates. *Crystals Growth and Design* **12**, 2917−2922 (2012).
77. Fang, J., Levchenko, I., Laan, T. van der, Kumar, S., Ostrikov, K. Multipurpose nanoporous alumina–carbon nanowall bi-dimensional nano-hybrid platform via catalyzed and catalyst-free plasma CVD. *Carbon* **78**, 627–632 (2014).
78. Han, Z. J. , Yick, S., Levchenko, I., Tam, E., Yajadda, M. M. A., Kumar, S., Martin, P. J., Furman, S., Ostrikov, K. Controlled synthesis of a large fraction of metallic single-walled carbon nanotube and semiconducting carbon nanowire networks. *Nanoscale* **3**, 3214-3220 (2011).
79. Kumar, S., Levchenko, I., Ostrikov, K. K., McLaughlin, J. A. Plasma-enabled, catalyst-free growth of carbon nanotubes on mechanically-written Si features with arbitrary shape. *Carbon* **50**, 325-329 (2012).
80. Levchenko, I., Ostrikov, K., Keidar, M., Xu, S. Deterministic nanoassembly: Neutral or plasma route? *Applied Physics Letters* **89**, 033109 (2006).

Figure 1

Click here to access/download;Figure;Figure 1(2).tiff

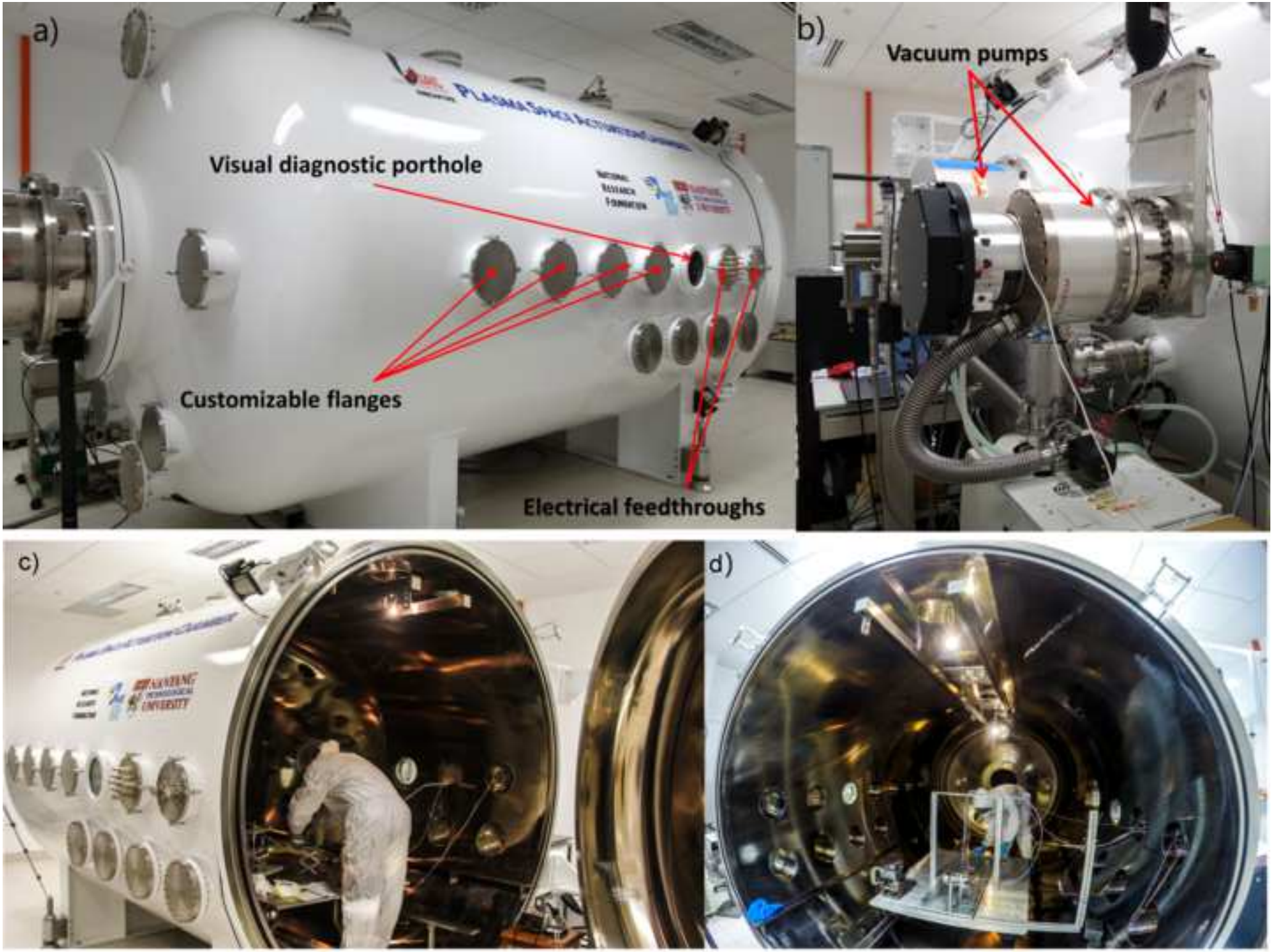

Click here to access/download;Figure;Figure 2.tiff

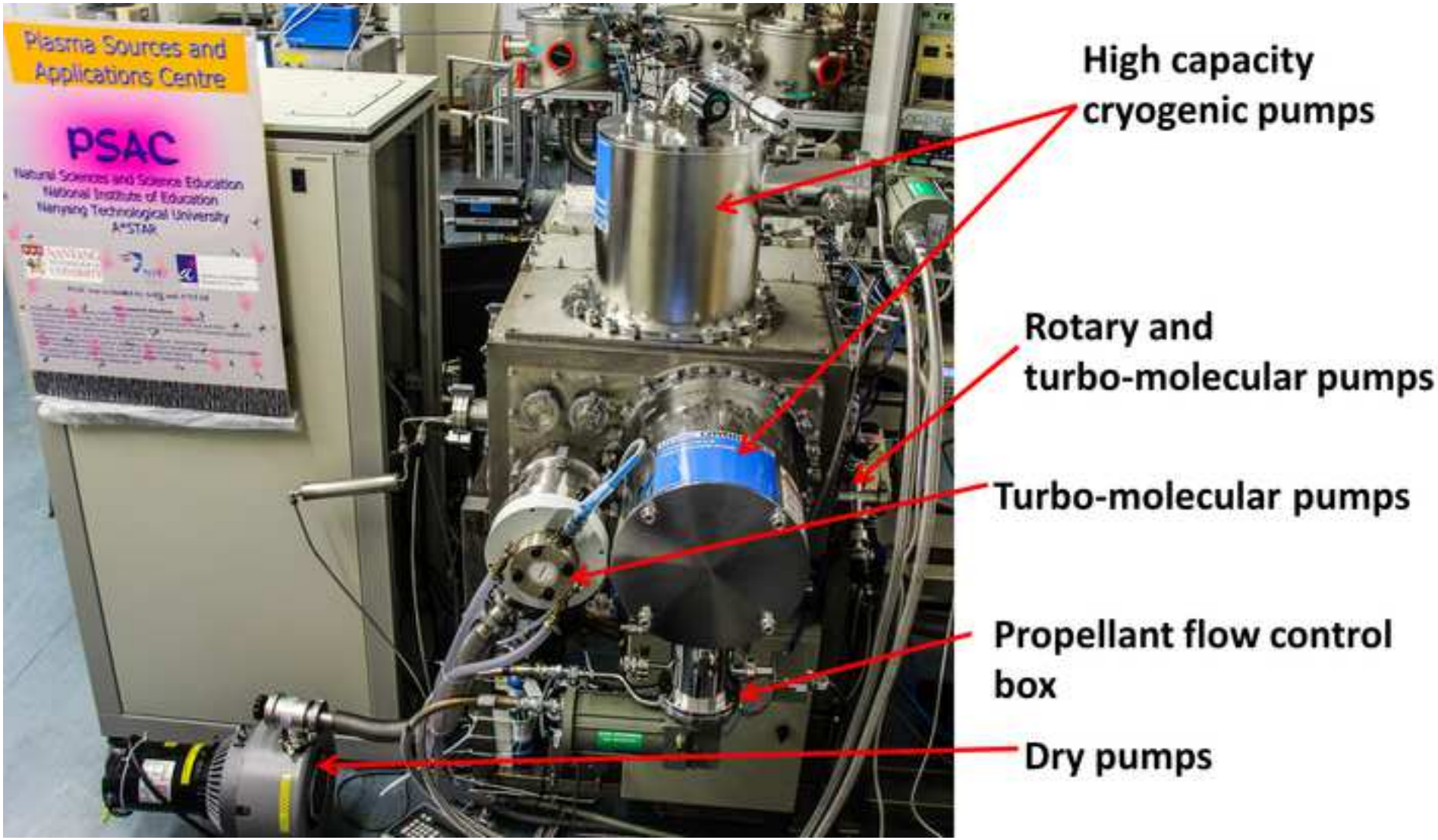

Click here to access/download;Figure;Figure 3.tiff

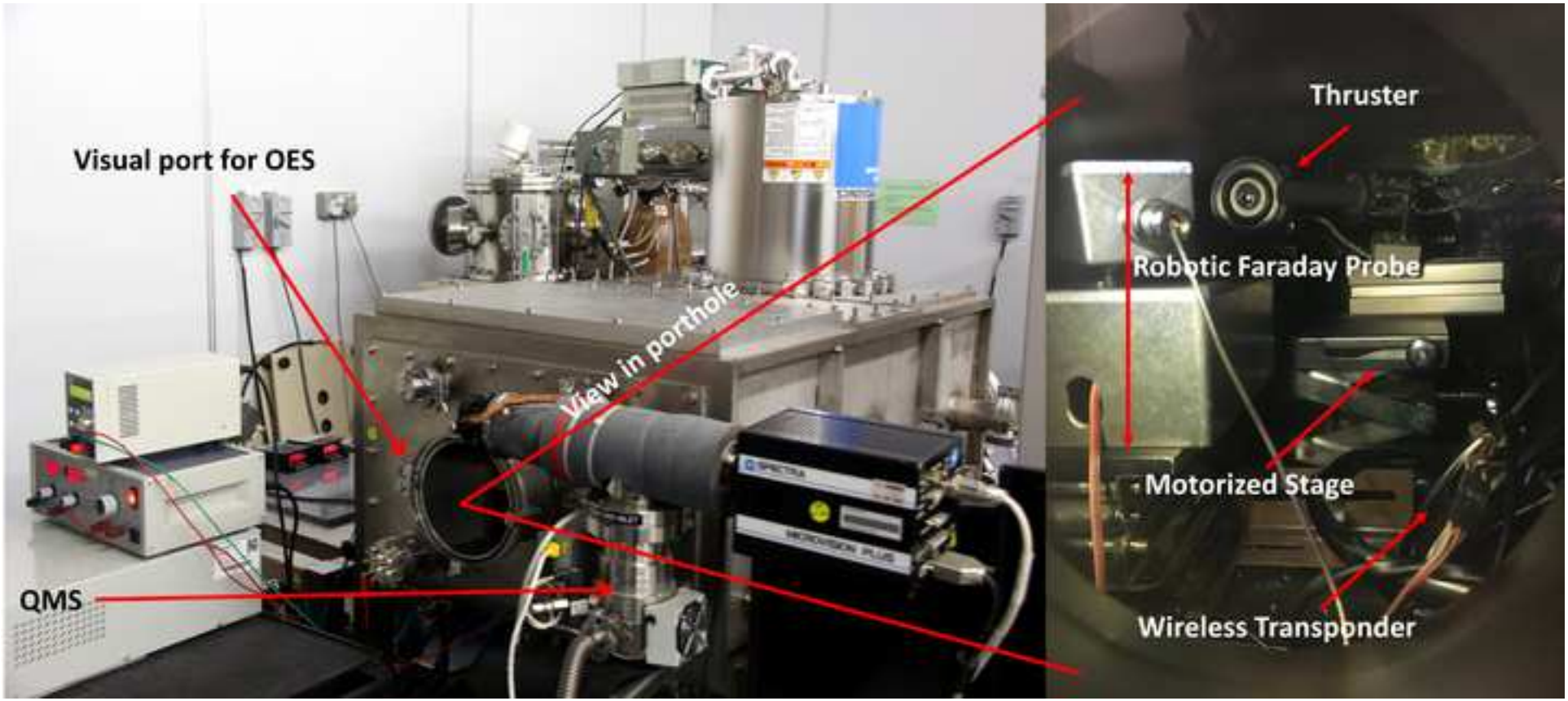

Figure 4

Click here to access/download;Figure;Figure 4(2).tiff

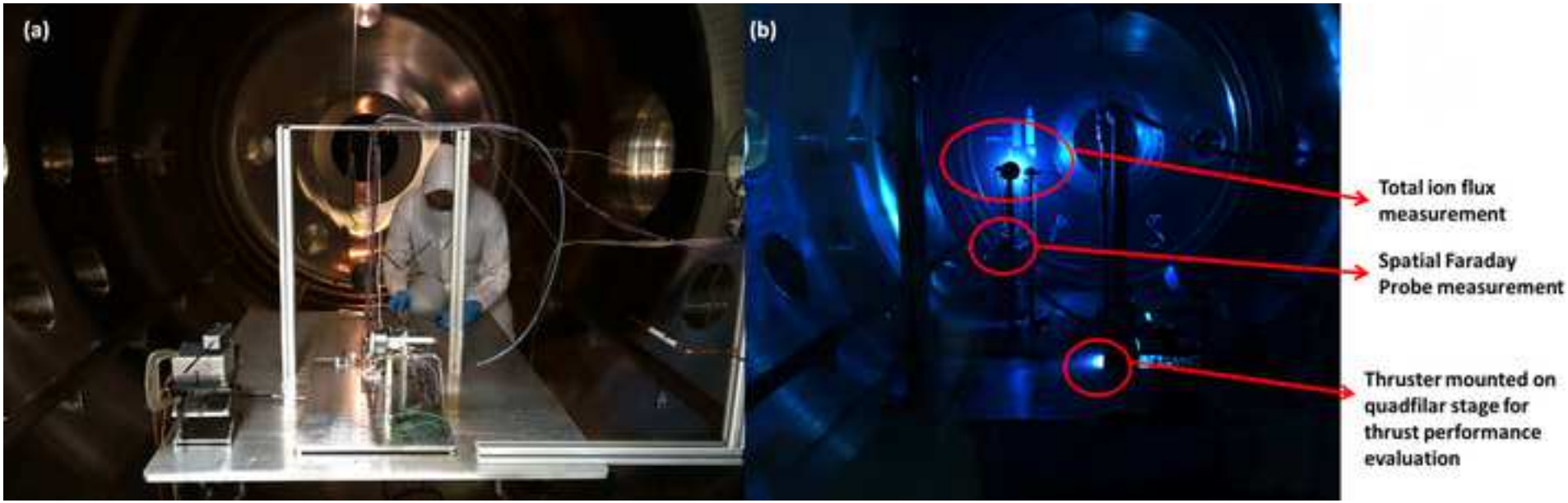

Click here to access/download;Figure;Figure 5.tiff

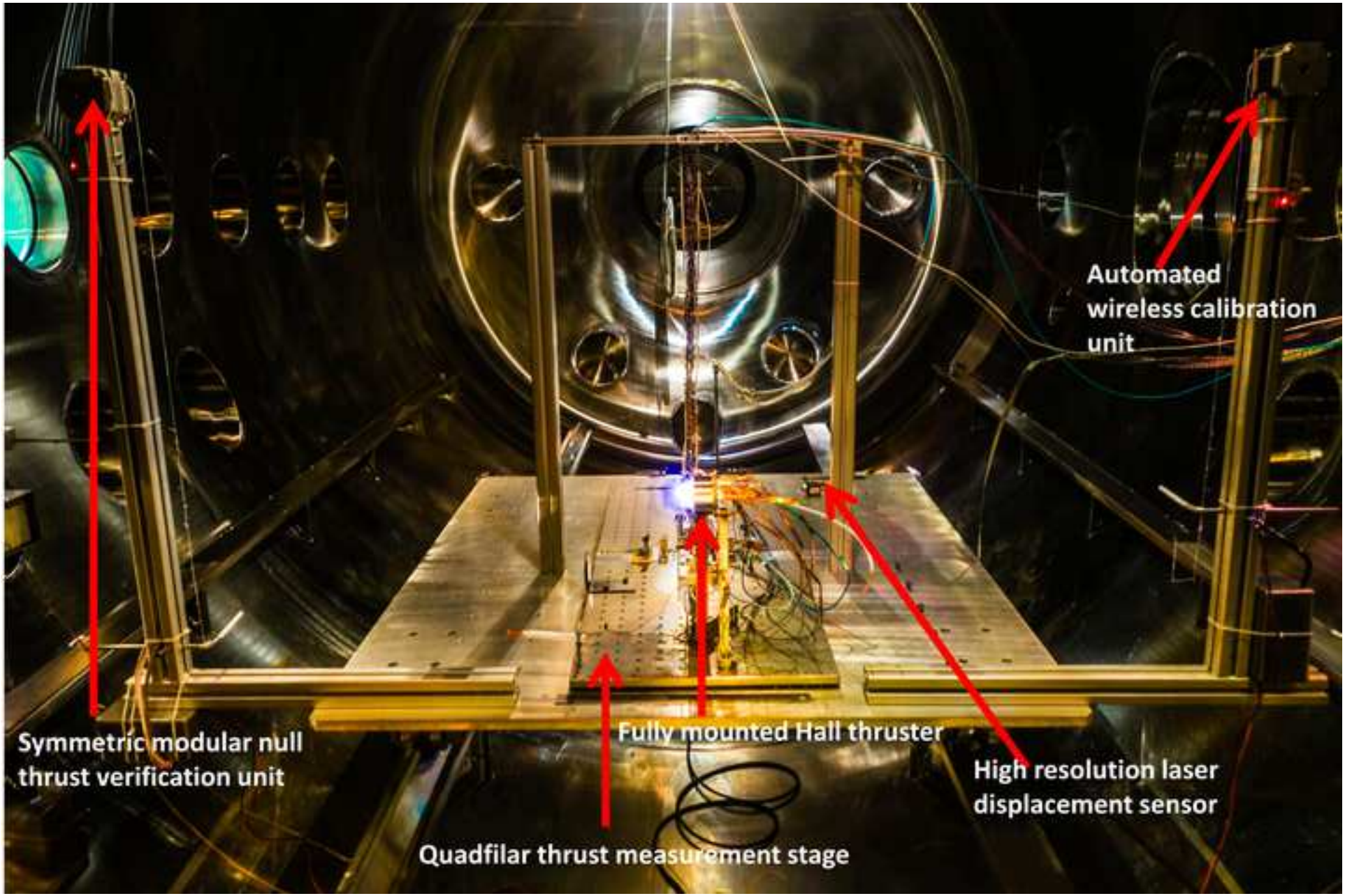

Click here to access/download;Figure;Figure 6.tiff

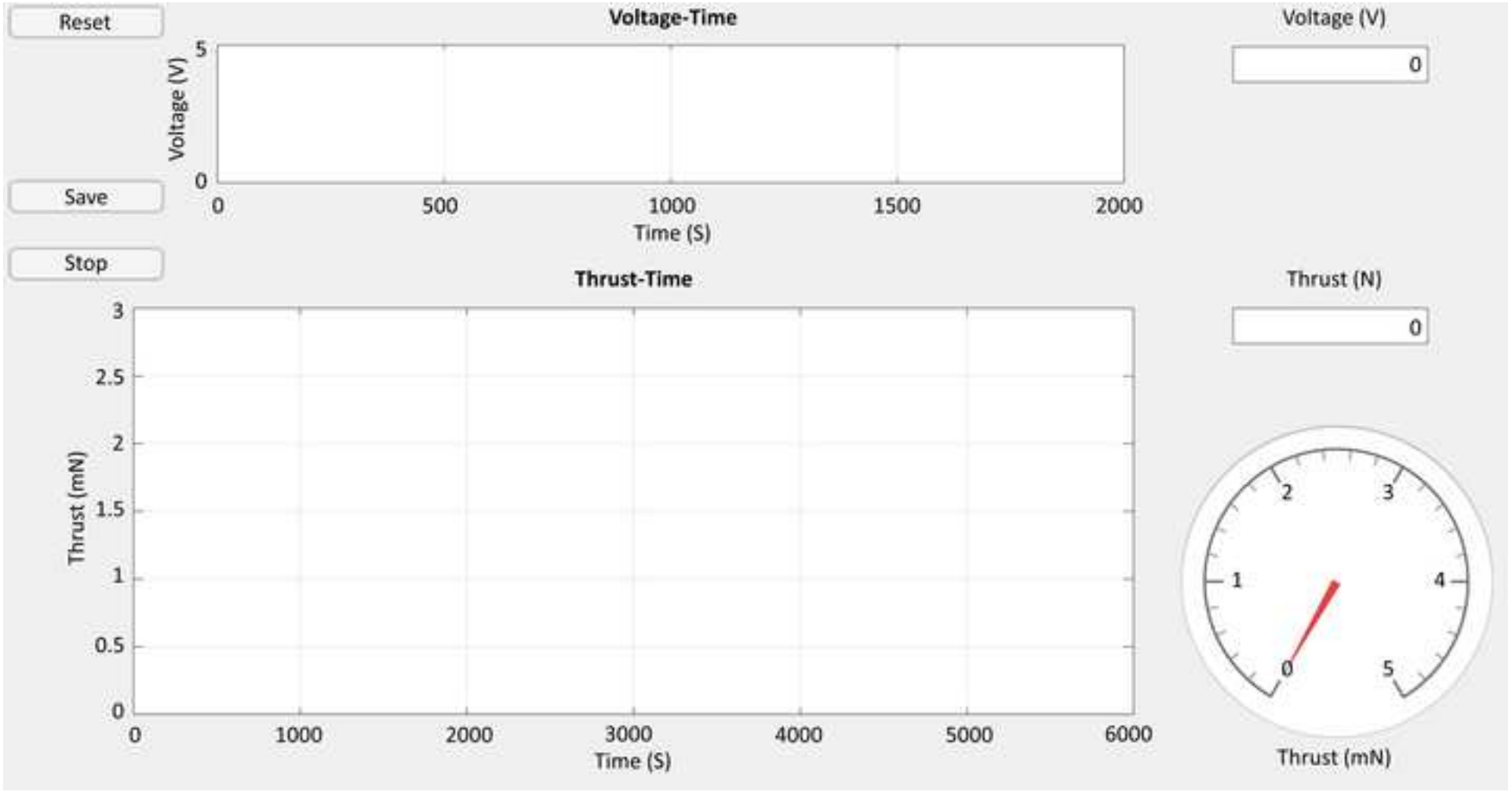

Figure 7

Click here to access/download;Figure;Figure 7(2).tiff

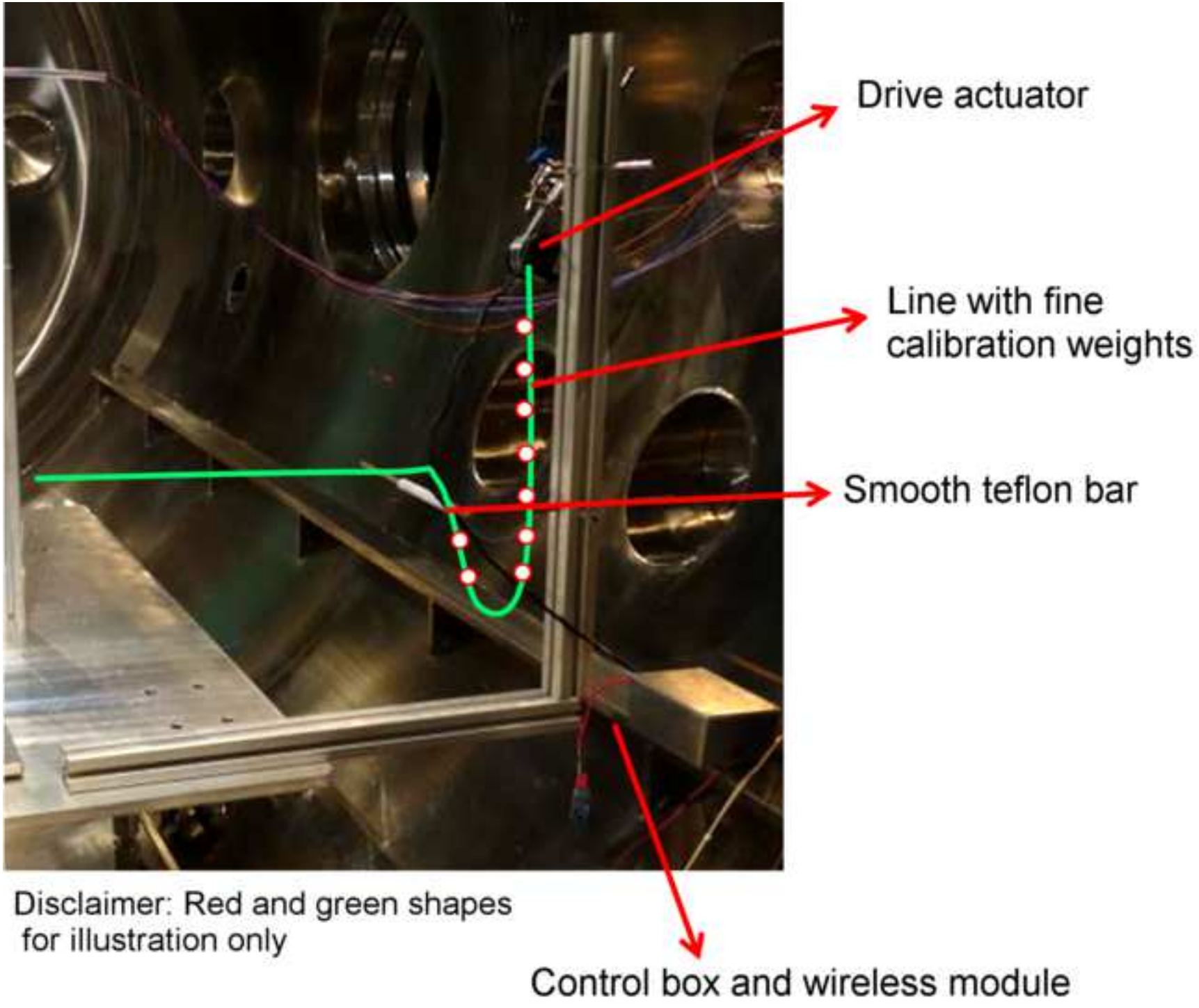

Click here to access/download;Figure;Figure 8.tiff

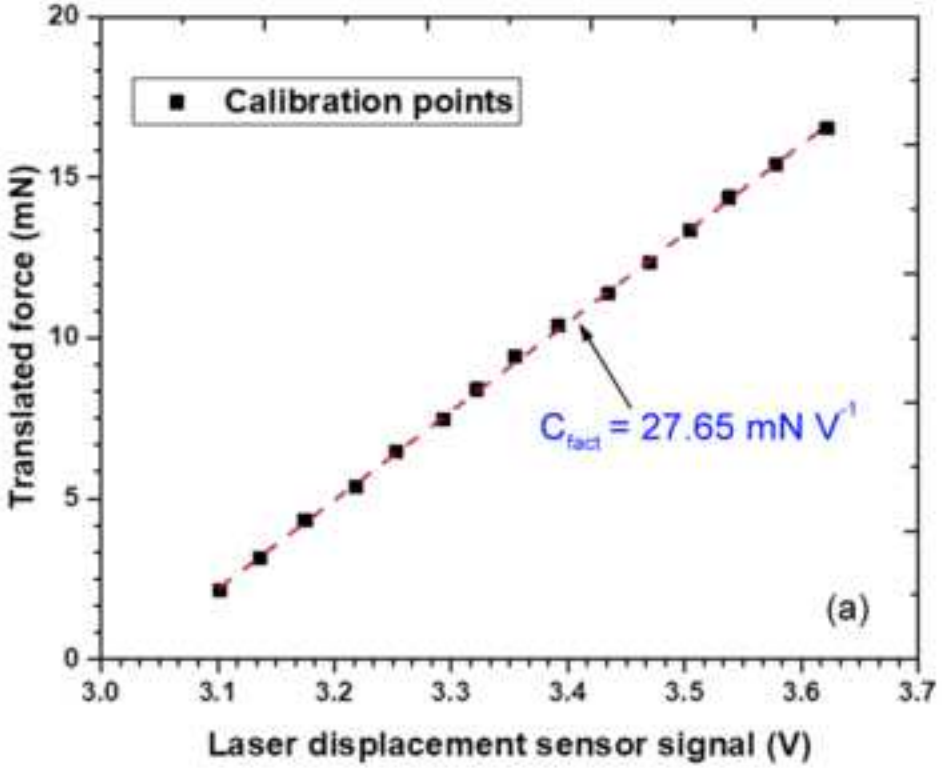

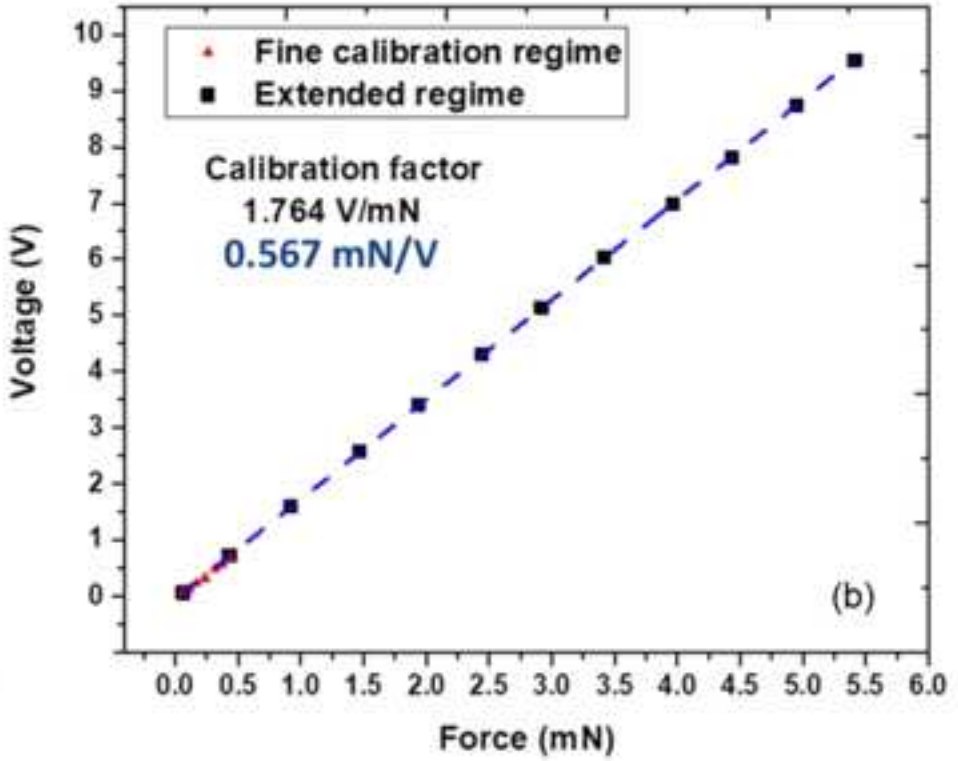

Click here to access/download;Figure;Figure 9.tiff

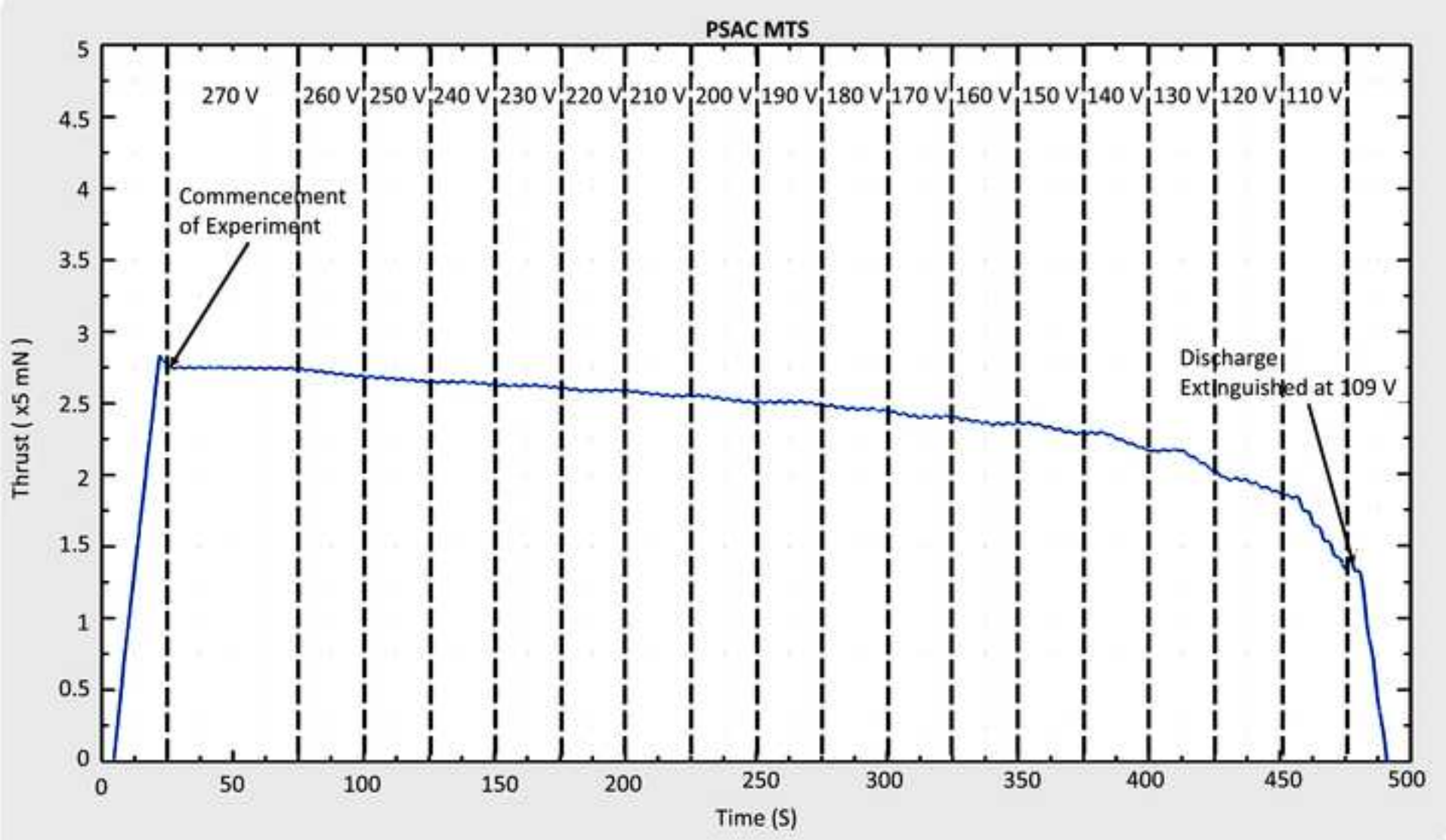

Click here to access/download;Figure;Figure 10.tiff

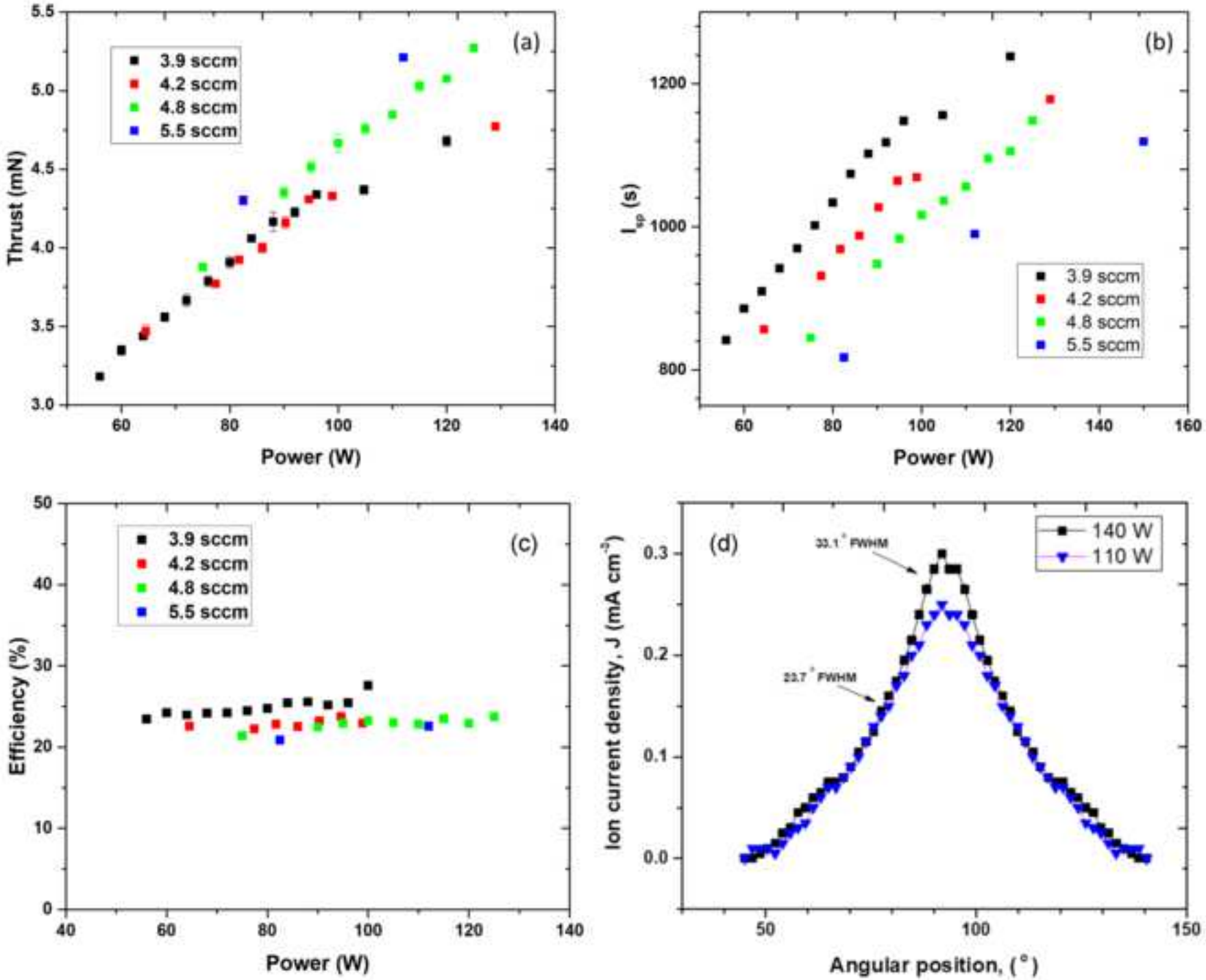

Click here to access/download;Figure;Figure 11.tiff

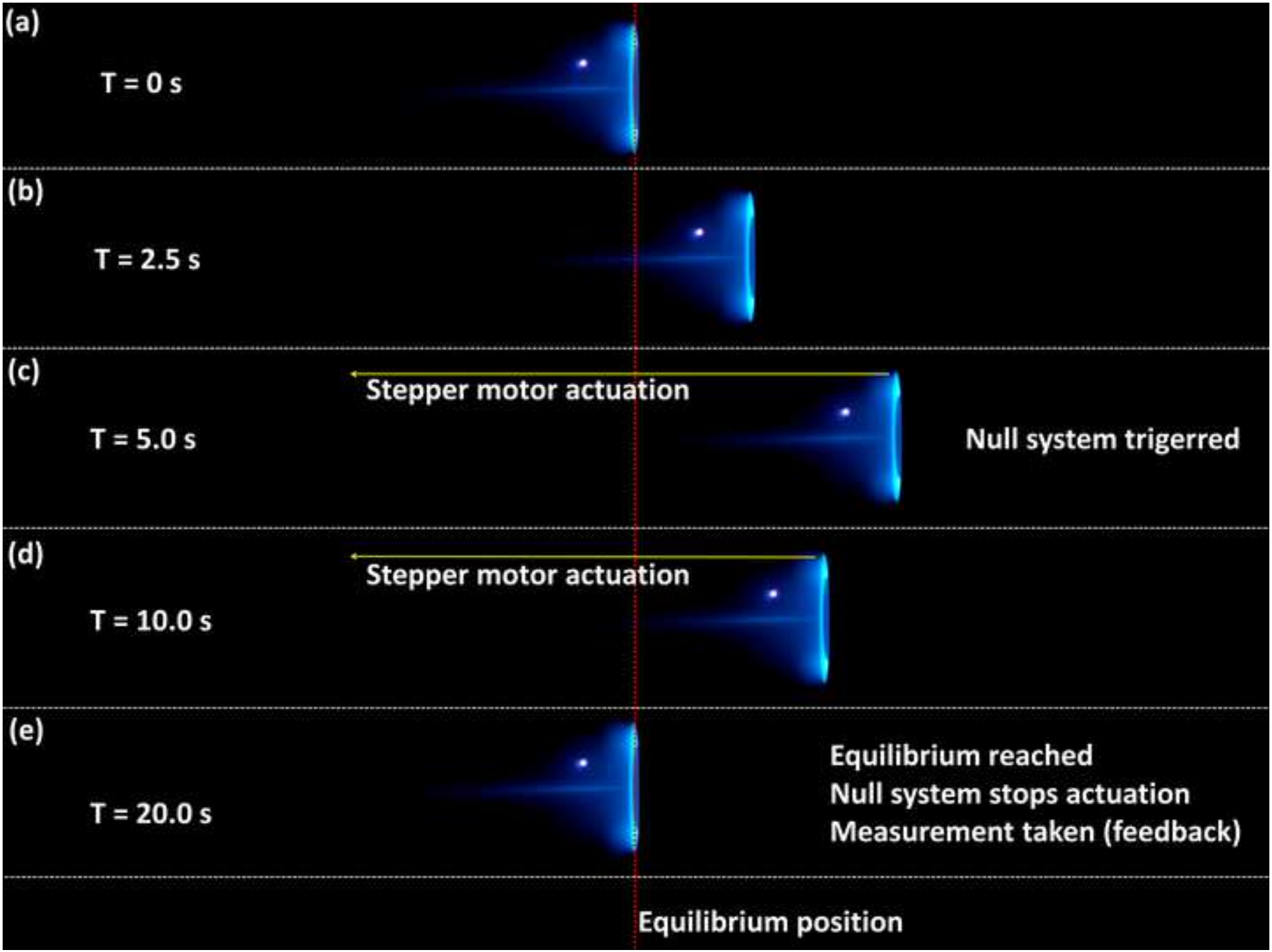

Click here to access/download;Figure;Figure 12.tiff

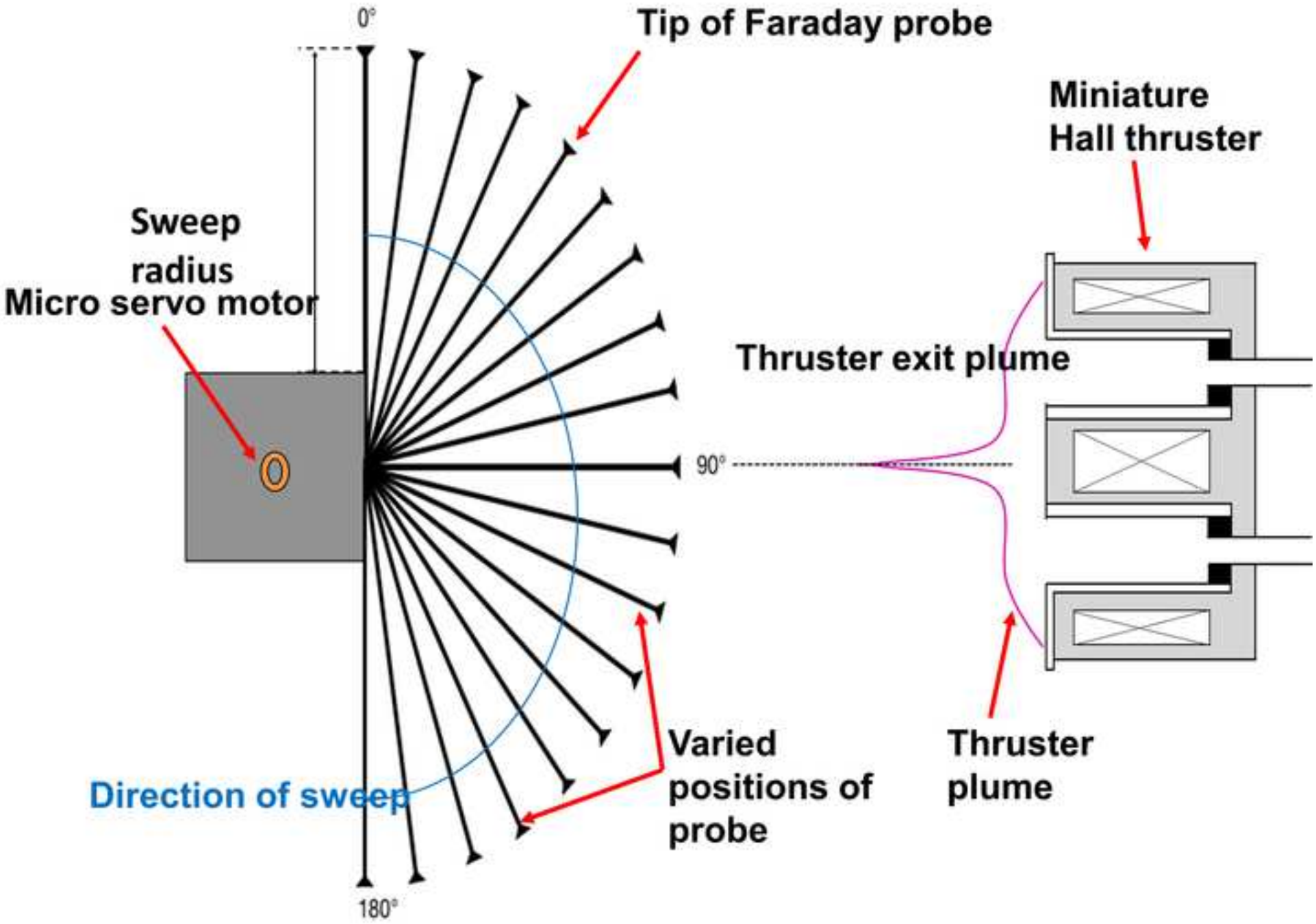

Click here to access/download;Figure;Figure 13.tiff

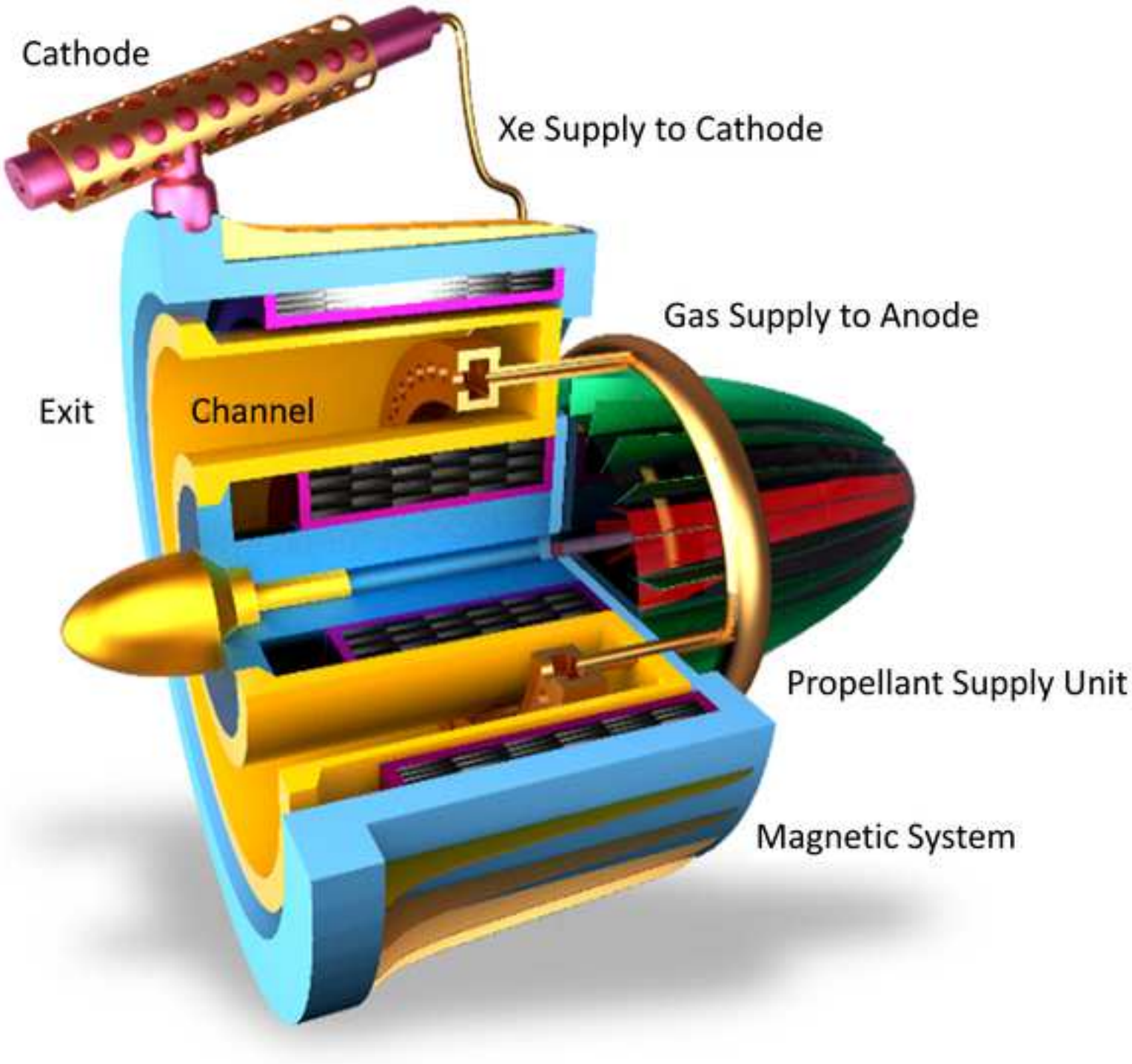

Click here to access/download;Figure;Figure 14.tiff

Table of Materials

Click here to access/download;Table of Materials;Table of essential supplies and equipment.xlsx

S/N	Name
1	Arduino Microcontroller
2	Bluetooth communication device
3	Cryogenic Pump
4	Digital Oscilloscope
5	Dry Pump
6	High resolution laser displacement sensor
7	Mass Flow Controller
8	Optical Emission Spectrometer
9	Servo Motor
10	Stepper Motor
11	Turbomolecular Pump

Company	Catalog number
Arduino	Arduino Uno Rev 3
SG Botic	WIR-02471
ULVAC	CRYO-U12HLE
Yokogawa	DLM 2054
Agilent	Triscroll-600
Micro-Epsilon	optoNCDT ILD-1420-50
MKS	MKS M100B
Avantes	AvaSpec-ULS2048XL-EVO
Tower Pro	Servo Motor SG90
Oriental Motor	PKP213D05A
Pfeiffer	ATH-500M

Author License Agreement (ALA)

Click here to access/download;Author License Agreement (ALA);Author_License_Agreement_Levchenko.pdf

jove JOURNAL OF VISUALIZED EXPERIMENTS

1 Alewife Center #200
Cambridge, MA 02140
tel. 617.945.9051
www.jove.com

ARTICLE AND VIDEO LICENSE AGREEMENT

Title of Article: Optimization, test and diagnostics of miniaturized Hall thrusters

Author(s): J. W. M. Lim, I. Levchenko, S. Huang, L. Xu, Y. F. Sun, G. C. Portrivitu, J.S. Yee, R. Z. W. Sim, Y. M. Wang, S. Levchenko, K. Bazaka, S. Xu

Item 1 (check one box): The Author elects to have the Materials be made available (as described at http://www.jove.com/author) via: [X] Standard Access [ ] Open Access

Item 2 (check one box):

[X] The Author is NOT a United States government employee.

[ ] The Author is a United States government employee and the Materials were prepared in the course of his or her duties as a United States government employee.

[ ] The Author is a United States government employee but the Materials were NOT prepared in the course of his or her duties as a United States government employee.

ARTICLE AND VIDEO LICENSE AGREEMENT

1. Defined Terms. As used in this Article and Video License Agreement, the following terms shall have the following meanings: "**Agreement**" means this Article and Video License Agreement; "**Article**" means the article specified on the last page of this Agreement, including any associated materials such as texts, figures, tables, artwork, abstracts, or summaries contained therein; "**Author**" means the author who is a signatory to this Agreement; "**Collective Work**" means a work, such as a periodical issue, anthology or encyclopedia, in which the Materials in their entirety in unmodified form, along with a number of other contributions, constituting separate and independent works in themselves, are assembled into a collective whole; "**CRC License**" means the Creative Commons Attribution-Non Commercial-No Derivs 3.0 Unported Agreement, the terms and conditions of which can be found at: http://creativecommons.org/licenses/by-nc-nd/3.0/legalcode; "**Derivative Work**" means a work based upon the Materials or upon the Materials and other pre-existing works, such as a translation, musical arrangement, dramatization, fictionalization, motion picture version, sound recording, art reproduction, abridgment, condensation, or any other form in which the Materials may be recast, transformed, or adapted; "**Institution**" means the institution, listed on the last page of this Agreement, by which the Author was employed at the time of the creation of the Materials; "**JoVE**" means MyJove Corporation, a Massachusetts corporation and the publisher of *The Journal of Visualized Experiments;* "**Materials**" means the Article and / or the Video; "**Parties**" means the Author and JoVE; "**Video**" means any video(s) made by the Author, alone or in conjunction with any other parties, or by JoVE or its affiliates or agents, individually or in collaboration with the Author or any other parties, incorporating all or any portion of the Article, and in which the Author may or may not appear.

2. Background. The Author, who is the author of the Article, in order to ensure the dissemination and protection of the Article, desires to have the JoVE publish the Article and create and transmit videos based on the Article. In furtherance of such goals, the Parties desire to memorialize in this Agreement the respective rights of each Party in and to the Article and the Video.

3. Grant of Rights in Article. In consideration of JoVE agreeing to publish the Article, the Author hereby grants to JoVE, subject to **Sections 4** and **7** below, the exclusive, royalty-free, perpetual (for the full term of copyright in the Article, including any extensions thereto) license (a) to publish, reproduce, distribute, display and store the Article in all forms, formats and media whether now known or hereafter developed (including without limitation in print, digital and electronic form) throughout the world, (b) to translate the Article into other languages, create adaptations, summaries or extracts of the Article or other Derivative Works (including, without limitation, the Video) or Collective Works based on all or any portion of the Article and exercise all of the rights set forth in (a) above in such translations, adaptations, summaries, extracts, Derivative Works or Collective Works and (c) to license others to do any or all of the above. The foregoing rights may be exercised in all media and formats, whether now known or hereafter devised, and include the right to make such modifications as are technically necessary to exercise the rights in other media and formats. If the "Open Access" box has been checked in **Item 1** above, JoVE and the Author hereby grant to the public all such rights in the Article as provided in, but subject to all limitations and requirements set forth in, the CRC License.

4. Retention of Rights in Article. Notwithstanding the exclusive license granted to JoVE in **Section 3** above, the Author shall, with respect to the Article, retain the non-exclusive right to use all or part of the Article for the non-commercial purpose of giving lectures, presentations or teaching classes, and to post a copy of the Article on the Institution's website or the Author's personal website, in each case provided that a link to the Article on the JoVE website is provided and notice of JoVE's copyright in the Article is included. All non-copyright intellectual property rights in and to the Article, such as patent rights, shall remain with the Author.

5. Grant of Rights in Video – Standard Access. This **Section 5** applies if the "Standard Access" box has been checked in **Item 1** above or if no box has been checked in **Item 1** above. In consideration of JoVE agreeing to produce, display or otherwise assist with the Video, the Author hereby acknowledges and agrees that, Subject to **Section 7** below, JoVE is and shall be the sole and exclusive owner of all rights of any nature, including, without limitation, all copyrights, in and to the Video. To the extent that, by law, the Author is deemed, now or at any time in the future, to have any rights of any nature in or to the Video, the Author hereby disclaims all such rights and transfers all such rights to JoVE.

6. Grant of Rights in Video – Open Access. This **Section 6** applies only if the "Open Access" box has been checked in **Item 1** above. In consideration of JoVE agreeing to produce, display or otherwise assist with the Video, the Author hereby grants to JoVE, subject to **Section 7** below, the exclusive, royalty-free, perpetual (for the full term of copyright in the Article, including any extensions thereto) license (a) to publish, reproduce, distribute, display and store the Video in all forms, formats and media whether now known or hereafter developed (including without limitation in print, digital and electronic form) throughout the world, (b) to translate the Video into other languages, create adaptations, summaries or extracts of the Video or other Derivative Works or Collective Works based on all or any portion of the Video and exercise all of the rights set forth in (a) above in such translations, adaptations, summaries, extracts, Derivative Works or Collective Works and (c) to license others to do any or all of the above. The foregoing rights may be exercised in all media and formats, whether now known or hereafter devised, and include the right to make such modifications as are technically necessary to exercise the rights in other media and formats. For any Video to which this Section 6 is applicable, JoVE and the Author hereby grant to the public all such rights in the Video as provided in, but subject to all limitations and requirements set forth in, the CRC License.

7. Government Employees. If the Author is a United States government employee and the Article was prepared in the course of his or her duties as a United States government employee, as indicated in **Item 2** above, and any of the licenses or grants granted by the Author hereunder exceed the scope of the 17 U.S.C. 403, then the rights granted hereunder shall be limited to the maximum rights permitted under such statute. In such case, all provisions contained herein that are not in conflict with such statute shall remain in full force and effect, and all provisions contained herein that do so conflict shall be deemed to be amended so as to provide to JoVE the maximum rights permissible within such statute.

8. Likeness, Privacy, Personality. The Author hereby grants JoVE the right to use the Author's name, voice, likeness, picture, photograph, image, biography and performance in any way, commercial or otherwise, in connection with the Materials and the sale, promotion and distribution thereof. The Author hereby waives any and all rights he or she may have, relating to his or her appearance in the Video or otherwise relating to the Materials, under all applicable privacy, likeness, personality or similar laws.

9. Author Warranties. The Author represents and warrants that the Article is original, that it has not been published, that the copyright interest is owned by the Author (or, if more than one author is listed at the beginning of this Agreement, by such authors collectively) and has not been assigned, licensed, or otherwise transferred to any other party. The Author represents and warrants that the author(s) listed at the top of this Agreement are the only authors of the Materials. If more than one author is listed at the top of this Agreement and if any such author has not entered into a separate Article and Video License Agreement with JoVE relating to the Materials, the Author represents and warrants that the Author has been authorized by each of the other such authors to execute this Agreement on his or her behalf and to bind him or her with respect to the terms of this Agreement as if each of them had been a party hereto as an Author. The Author warrants that the use, reproduction, distribution, public or private performance or display, and/or modification of all or any portion of the Materials does not and will not violate, infringe and/or misappropriate the patent, trademark, intellectual property or other rights of any third party. The Author represents and warrants that it has and will continue to comply with all government, institutional and other regulations, including, without limitation all institutional, laboratory, hospital, ethical, human and animal treatment, privacy, and all other rules, regulations, laws, procedures or guidelines, applicable to the Materials, and that all research involving human and animal subjects has been approved by the Author's relevant institutional review board.

10. JoVE Discretion. If the Author requests the assistance of JoVE in producing the Video in the Author's facility, the Author shall ensure that the presence of JoVE employees, agents or independent contractors is in accordance with the relevant regulations of the Author's institution. If more than one author is listed at the beginning of this Agreement, JoVE may, in its sole discretion, elect not take any action with respect to the Article until such time as it has received complete, executed Article and Video License Agreements from each such author. JoVE reserves the right, in its absolute and sole discretion and without giving any reason therefore, to accept or decline any work submitted to JoVE. JoVE and its employees, agents and independent contractors shall have

full, unfettered access to the facilities of the Author or of the Author's institution as necessary to make the Video, whether actually published or not. JoVE has sole discretion as to the method of making and publishing the Materials, including, without limitation, to all decisions regarding editing, lighting, filming, timing of publication, if any, length, quality, content and the like.

11. Indemnification. The Author agrees to indemnify JoVE and/or its successors and assigns from and against any and all claims, costs, and expenses, including attorney's fees, arising out of any breach of any warranty or other representations contained herein. The Author further agrees to indemnify and hold harmless JoVE from and against any and all claims, costs, and expenses, including attorney's fees, resulting from the breach by the Author of any representation or warranty contained herein or from allegations or instances of violation of intellectual property rights, damage to the Author's or the Author's institution's facilities, fraud, libel, defamation, research, equipment, experiments, property damage, personal injury, violations of institutional, laboratory, hospital, ethical, human and animal treatment, privacy or other rules, regulations, laws, procedures or guidelines, liabilities and other losses or damages related in any way to the submission of work to JoVE, making of videos by JoVE, or publication in *JoVE* or elsewhere by JoVE. The Author shall be responsible for, and shall hold JoVE harmless from, damages caused by lack of sterilization, lack of cleanliness or by contamination due to the making of a video by JoVE its employees, agents or independent contractors. All sterilization, cleanliness or decontamination procedures shall be solely the responsibility of the Author and shall be undertaken at the Author's expense. All indemnifications provided herein shall include JoVE's attorney's fees and costs related to said losses or damages. Such indemnification and holding harmless shall include such losses or damages incurred by, or in connection with, acts or omissions of JoVE, its employees, agents or independent contractors.

12. Fees. To cover the cost incurred for publication, JoVE must receive payment before production and publication the Materials. Payment is due in 21 days of invoice. Should the Materials not be published due to an editorial or production decision, these funds will be returned to the Author. Withdrawal by the Author of any submitted Materials after final peer review approval will result in a US$1,200 fee to cover pre-production expenses incurred by JoVE. If payment is not received by the completion of filming, production and publication of the Materials will be suspended until payment is received.

13. Transfer, Governing Law. This Agreement may be assigned by JoVE and shall inure to the benefits of any of JoVE's successors and assignees. This Agreement shall be governed and construed by the internal laws of the Commonwealth of Massachusetts without giving effect to any conflict of law provision thereunder. This Agreement may be executed in counterparts, each of which shall be deemed an original, but all of which together shall be deemed to me one and the same agreement. A signed copy of this Agreement delivered by facsimile, e-mail or other means of electronic transmission shall be deemed to have the same legal effect as delivery of an original signed copy of this Agreement.

A signed copy of this document must be sent with all new submissions. Only one Agreement required per submission.

CORRESPONDING AUTHOR:

Name:	Igor Levchenko
Department:	Plasma Sources and Applications Centre
Institution:	Nanyang Technological University
Article Title:	Optimization, test and diagnostics of miniaturized Hall thrusters
Signature:	I.Levchenko
Date:	14 May 2018

Please submit a signed and dated copy of this license by one of the following three methods:

1) Upload a scanned copy of the document as a pfd on the JoVE submission site;
2) Fax the document to +1.866.381.2236;
3) Mail the document to JoVE / Attn: JoVE Editorial / 1 Alewife Center #200 / Cambridge, MA 02139

For questions, please email submissions@jove.com or call +1.617.945.9051

Rebuttal Letter
Click here to access/download;Rebuttal Letter;JoVE58466R2-Cover.pdf

Prof. Dr. Igor Levchenko

Plasma Sources and Applications Centre / Space Propulsion Centre Singapore
Nanyang Technological University
and
School of Chemistry, Physics, and Mechanical Engineering
Queensland University of Technology, Australia
levchenko.igor@nie.edu.sg
Igor.Levchenko@qut.edu.au
I.Levchenko@post.com

14 November 2018

Dear Editor,

Re: Revised manuscript JoVE58466

Please find uploaded our revised manuscript JoVE58466 "***Optimization, test and diagnostics of miniaturized Hall thrusters***" by J. W. M. Lim, I. Levchenko, M. W. A. B. Rohaizat, S. Huang, L. Xu, Y. F. Sun, G. C. Portrivitu, J. S. Yee, R. Z. W. Sim, Y. M. Wang, S. Levchenko, K. Bazaka and S. Xu.

All the valuable comments and suggestions of the Reviewers and the Editor have been thoroughly taken into consideration and addressed in the revised manuscript.

We thank the Reviewers and the Editorial Office for their time, constructive criticism and valuable suggestions, and hope that the revised manuscript is now suitable for publication in ***2D Materials*.**

Appended is a comprehensive list of revisions suggested by the Editor and Reviewers, and our responses/amendments in the manuscript.

Yours sincerely,

Igor Levchenko

Response to the comments and suggestions of the Editors and Reviewers with the detailed list of revisions made

_____

Editorial and production comments:

Comment: 1*. Please take this opportunity to thoroughly proofread the manuscript to ensure that there are no spelling or grammar issues. The JoVE editor will not copy-edit your manuscript and any errors in the submitted revision may be present in the published version.*

Response: We thank the Editors for careful checking our manuscript. We have thoroughly proofread our work and believe it is fine now.

Comment: 2. *Please use American English throughout.*

Response: American English is now used throughout our manuscript.

Comment: 3. *Unfortunately, there are a few sections of the manuscript that show overlap with previously published work. Though there may be a limited number of ways to describe a technique, please use original language throughout the manuscript. Please see lines: the first 7 lines of the Abstract.*

Response: We have checked and rephrased the manuscript to make the text original.

Comment: 4. *Please remove the embedded figure(s) from the manuscript. All figures should be uploaded separately to your Editorial Manager account. Each figure must be accompanied by a title and a description after the Representative Results of the manuscript text.*

Response: We have removed the images and uploaded them as separate tiff files. A separate file with the descriptions is also uploaded.

Comment: Please submit the figures as a vector image file to ensure high resolution throughout production: (.svg, .eps, .ai). If submitting as a .tif or .psd, please ensure that the image is 1920 pixels x 1080 pixels or 300dpi.

Response: We have uploaded the images as separate tiff files with the resolutions not less than 300 and pixel sizes of about 3000.

Comment: *Please reduce the number of figures if possible. Some can be combined to be different panels of the same Figure number*.

Response: We have re-grouped and combined several images, thus the total number was reduced to 14.

Comment: *Please do not abbreviate journal references.*

Response: We have spelled out all references.

Comment: *Please define all abbreviations before use.*

Response: All abbreviations are now defined.

Comment: *Please revise the table of the essential supplies, reagents, and equipment. The table should include the name, company, and catalog number of all relevant materials in separate columns in an xls/xlsx file. Please sort the Materials Table alphabetically by the name of the material.*

Response: Revised Materials Table was uploaded.

Comment: *Please include a Summary that clearly describes the protocol and its applications in complete sentences between 10-50 words: "Here, we present a protocol to …"*

Response: Summary was included to describe the protocol:

Here, we present a protocol to test and optimize miniaturized space propulsion systems. Diversified sophisticatedly designed equipment, large vacuum chambers, powerful pumping platforms and various diagnostic complexes were used to perform precise, informative characterization of micro-propulsion thrusters under conditions close to those found in open space. Skilled personnel, adequate simulation and theoretical support are also of key importance to keep the micropropulsion design and technology progressing steadily. Development of novel materials is the second key factor that could ensure significant breakthroughs in improving performance characteristics of modern electric propulsion systems, including small satellites and CubeSats with the whole set of supply systems, peripheral instruments, tools and payload.

Comment: *Please ensure that the Abstract is under 300 words.*

Response: The Abstract length is now under 300 words (277).

Comment: *Please place the superscripted numbered reference before the punctuation.*

Response: This was corrected, the superscripted numbered reference are now before the punctuation marks.

Comment: *Please do not number the paragraphs in the Introduction.*

Response: Numbering was removed in the Introduction of the revised manuscript.

Comment: *Please use complete sentences throughout the introduction and avoid lists.*

Response: Lists were removed in the Introduction of the revised manuscript. Complete sentences are used now.

Comment: *Please end each sentence and protocol step with a period.*

Response: Periods were added where appropriate, including protocol steps, in the revised manuscript.

Comment: *Please add more details to your protocol steps. Please ensure you answer the "how" question, i.e., how is the step performed? Alternatively, add references to published material specifying how to perform the protocol action.*

Response: The protocol was significantly re-developed and extended to address these comments.

Comment: *1.6: What weight is used?*

Response: The weight used was a precisely known and calibrated mass of copper loop. The mass of each copper loop depends on the intended sensitivity of the quadfilar stage being used. In this case, the mass of each copper loop was in the order of 100 mg for the extended calibration regime and 10 mg for the fine calibration regime. We have added this information in the revised version, page 4. See the representative results for more information on how the weights were used to find out the quadfilar thrust sensitivity.

Comment: *For all computational steps, please provide all user input commands: File | Save | etc.*

Response: These steps were added in the protocol. Mainly, they are the procedures of opening and closing files, i.e. quite apparent steps. Nevertheless, we have added this information, where appropriate.

Comment: Please provide all experimental and operational parameters throughout. We need specific values and numbers rather than a generalized protocol. What is the desired vacuum, etc.?

Response: All this information was added in the significantly extended protocol (i.e., $<10^{-5}$ Pa).

Comment: *We respect the confidentiality of some of the experimental design but please provide some more information so that others can replicate the protocol itself.*

Response: We have extended the protocol and added the information, and we believe the protocol is now quite reproducible.

We thank the Editorial for these very useful comments, and believe the manuscript is now at the level of the JoVE's high standards.

Changes to be made by the Author(s) regarding the video:

1. Please ensure that the additional details above are reflected in the video as well.

2. Please increase the homogeneity between the written protocol text and the video narration. For example, the step 1 title is different in the video and the written protocol, protocol steps itself, etc.

3. Frame size/proportions issues

• 1:05-1:12 - Ideally, this image would fill the frame with no black or white borders. If that is impossible, the white background should be extended to fill the black borders on the left and right of frame.

• 7:40-7:48 - Rather than a slow zoom in on this image, we would recommend having it fill the frame and keeping it still. It will likely be of more use to the audience that way.

• 10:09-10:18 - This video needs to fill the frame. It would need to be reshot. Or, you could do what a lot of news shows do for vertical cell phone video: duplicate and enlarge the video, place the enlarged clip behind the original clip, and blur the enlarged clip. The process is described here: https://www.youtube.com/watch?v=LdCLQ2DQ0NY. This would make the square video seem more intentional and integrate it better with the rest of the video.

4. Editing issues

• 3:22, 3:41, 3:43, 4:06, 7:23, 7:52, 8:25, 8:46 - There is a blank frame in the middle of the edits at the listed times. This should be corrected.

• 3:19, 3:54 - The edits here are jump cuts (https://en.wikipedia.org/wiki/Jump_cut), which tend to have a jarring effect on the viewer. They should be smoothed out with crossfades instead.

• 3:44-3:56 - This is a still shot of the apparatus that slowly zooms in. The image then jump cuts back to its original position at 3:54. The zooming motion also leads to the positioning of the on-screen text label to become misplaced. We would recommend using a still image of the apparatus that does not zoom in.

• 7:52-7:53 - This edit needs to be fixed. The video cuts to black with the text still on screen, then to a frame or two of Sun Yufei's interview, before moving on to the next clip.

5. Video quality issues

• 5:28-5:36 - This shot is overly shaky. Since no important action is happening in the shot, we would recommend using a still frame from this video clip in place of the live-action video clip itself.

6. Branding concerns

• 2:18 - There is a logo here for PSAC; logos, even for non-commercial entities, should be removed from the body of the Protocol.

7. Please show the beginning title card at the end as well.

Please upload a revised high-resolution video here: https://www.jove.com/account/file-uploader?src=17832178

We thank the JoVE's video team these suggestions, all of which were carefully implemented in the revised video, uploaded with the revised version of the manuscript.

Reviewers' comments:

Reviewer #1:

Comment: *This manuscript mainly introduced how to build, test, and optimize a small Hall thruster (30mm) suitable for a small satellite of about 50 kg. It also shows the thruster operating in a large space environment simulator, and describes how thrust is measured and electric parameters, including plasma characteristics, are collected and processed to assess key thruster parameters. This work is meaningful, and I support this work, and believe it's worth of publishing after some amendments.*

Response: We thank the Reviewer for the encouraging assessment of our work. We have thoroughly implemented all the suggestions to enhance our work.

Comment 1. *In the abstract of this paper, the authors state that they will also address challenges and opportunities presented by new thruster materials. However, there is no research and experiment on new materials in this paper. It just summarizes previous research results and describes the current research status in the discussion part, I think it is necessary add a part about the thruster materials.*

Response: Thanks for this suggestion. This paper does not directly address the thruster materials issues, but is related to the equipment which could be used for the materials testing and technological plasma diagnostics, and on the other hand, it deals with the diagnostics of thruster behavior when some novel materials are applied. Due to the limited format of this work, we cannot include the material related protocol but we added a short sub-section stating the material issues in thrusters, and added some more relevant references, such as:

Levchenko, I., Keidar, M., Cantrell, J., Wu, Y.-L., Kuninaka, H., Bazaka K. & Xu, S. Explore space using swarms of tiny satellites. *Nature* **562**, 185 (2018).

Levchenko, I., Bazaka, K., Ding, Y., Raitses, Y., Mazouffre, S., Henning, T., Klar, P. J. *et al*. Space micropropulsion systems for Cubesats and small satellites: from proximate targets to furthermost frontiers. *Applied Physics Reviews* **5**, 011104 (2018).

Levchenko, I., Bazaka, K., Belmonte, T., Keidar, M. & Xu, S. Advanced Materials for Next Generation Spacecraft. *Advanced Materials* **30**, 1802201 (2018).

Bazaka, K., Baranov, O., Cvelbar, U., Podgornik, B., Wang, Y., Huang, S., Xu, L., Lim, J. W. M., Levchenko, I. & Xu, S. Oxygen plasmas: a sharp chisel and handy trowel for nanofabrication. *Nanoscale* **10**, 17494-17511 (2018).

Comment 2. *In the representative results section, the Figure 7 and Figure 11 are not clear. To make this paper better understood, these two figures should be replaced.*

Response: Thank you, we have significantly enhanced, re-developed and re-grouped the illustrations.

Comment 3. *The author claims that they also demonstrate how the thruster is optimized to make it one of the most efficient small thrusters ever built. As a matter of fact, optimization requires a reference standard, and experimental data is required to indicate which aspects have been optimized, as well as the comparison of some important performances of the thruster before and after optimization. The thrust, specific impulse, power and efficiency should be added with figures or tables.*

Response: Thank you, we have added this information and have better shown the thruster parameters in the updated images.

Comment 4. *The author states that the new system can allow for up to 3 different thrusters to be mounted and tested simultaneously in the section 2.2. It is no doubt that it can reduce operational downtime and maximizing research output. However, how to make sure that these three different thrusters don't interact with each other?*

Response: Thanks for this insightful comment.

The thrusters can be mounted vertically in a single column and tested rapidly, one after another to avoid interactions between the different thruster systems. It has been verified that efficient evaluation of up to 3 different modules at a single instance is possible, thus significantly reducing the downtime during evacuation and purging processes required otherwise when testing systems individually. On the other hand, this system is a valuable opportunity for testing the thruster assemblies that should operate in a bunch, on the same satellite.

We have added a comment about this in the revised manuscript.

Comment 5. *I recommend adding the following recently publications about low power hall thruster (especially about permanent magnet and graphite channel wall):*

(1) Ding Yongjie, Li Hong, Sun Hezhi, Wei Liqiu, Jia Boyang, Su Hongbo, Peng Wuji, Li Peng, Yu Daren. A 200-W Permanent Magnet Hall Thruster Discharge with Graphite Channel Wall. Physics Letter A. 2018, 382, pp.3079-3082.

(2) Lou Grimaud, Stéphane Mazouffre. Performance comparison between standard and magnetically shielded 200 W Hall thrusters with BN-SiO2 and graphite channel walls. Vacuum, 2018,155,pp.514-523

(3) Ding Yongjie, Li Hong, Li Peng, Jia Boyang, Wei Liqiu, Su Hongbo, Sun Hezhi, Wang Lei, Yu Daren. Effect of Relative Position between Cathode and Magnetic Separatrix on the Discharge Characteristic of Hall Thrusters. Vacuum. 2018, 154,167-173.

(4) Stéphane Mazouffre, Lou Grimaud. Characteristics and Performances of a 100-W Hall Thruster for Microspacecraft. IEEE Transactions on Plasma Science. 46(2),pp.330-337.

(5) Ding Yongjie, Peng Wuji, Sun Hezhi, Wei Liqiu, Zeng Ming, Wang Fufeng, Yu Daren, Performance characteristics of No-Wall-Losses Hall thruster, The European Physical Journal - Special Topics, 2017, 226, 2945-2953

(6) Ding Yongjie, Sun Hezhi, Li Peng, Wei Liqiu, Su Hongbo, Peng Wuji, Li Hong, Yu Daren, Application of Hollow Anode in Hall Thruster with Double-peak Magnetic Fields, Journal of Physics D: Applied Physics, 2017, 50(33), 335201.

(7) Ryan W. Conversano, Dan M. Goebel, Richard R. Hofer and Ioannis G. Mikellides.Performance Analysis of a Low-Power Magnetically Shielded Hall Thruster: Experiments. Propulsion and Power, Vol. 33, No. 4 (2017), pp. 975-983.

(8) Ryan W. Conversano, Dan M. Goebel, Ioannis G. Mikellides and Richard R. Hofer. Performance Analysis of a Low-Power Magnetically Shielded Hall Thruster: Computational Modeling.Journal of Propulsion and Power, Vol. 33, No. 4 (2017), pp. 992-1001.

(9) Ding Yongjie, Sun Hezhi, Li Peng, Wei Liqiu, Xu Yu, Peng Wuji, Su Hongbo, Daren Yu, Influence of Hollow Anode Position on the Performance of a Hall-Effect Thruster with Double-peak Magnetic Field, Vacuum, 2017, 143, 251-261.

(10) Ding Yongjie, Peng Wuji, Sun Hezhi, Xu Yu, Wei Liqiu, Li Hong, Zeng Ming, Wang Fufeng, Yu Daren, Effect of oblique channel on discharge characteristics of 200-W Hall thruster, Physics of Plasmas, 2017, 24(2): 023507.

(11) Ding Yongjie, Peng Wuji, Sun Hezhi, Wei Liqiu, Zeng Ming, Wang Fufeng, Yu Daren, Visual evidence of suppressing the ion and electron energy loss on the wall in Hall thrusters, Japanese Journal of Applied Physics, 2017, 56(3): 038001.

(12) Ding Yongjie, Peng Wuji, Wei Liqiu, Sun Guoshun, Li Hong, Yu Daren, Computer simulations of Hall thrusters without wall losses designed using two permanent magnetic rings, Journal of Physics D: Applied Physics, 2016, 49(46): 465001.

Response: All these references have been added in the revised manuscript, with the total number of references exceeding 80 now.

Reviewer #2:

Comment: *There is no gross defect in this paper. But I get some advice for the author. Minor Concerns: The first one is about arranging your text and your figures. Figure 15 should be adjacent to the paragraph "Typical Hall-type thrusters are relatively simple".*

Second, could you please focus on optimization of Hall thruster more rather than facility. If you can provide improvement of Hall thruster in figure 16 instead of your facility, it would be better.

Response: Thank you for your suggestions.

In the revised version, we have significantly enhanced, re-developed and re-grouped the protocol, illustration and the general paper flow. Many additional information and references have been added. We believe the manuscript was now considerable enhanced, due to valuable criticism and suggestions of the Reviewers.

We thank again the JoVE's Editorial, video team and Reviewers, and believe the revised manuscript may be now accepted for publication.